

https://doi.org/10.1093/femsec/fiab103 Advance Access Publication Date: 0 2021 Research Article

#### RESEARCH ARTICLE

# Deep-sea hydrothermal vent sediments reveal diverse fungi with antibacterial activities

Emma Keeler<sup>1</sup>, Gaëtan Burgaud<sup>2</sup>, Andreas Teske<sup>3</sup>, David Beaudoin<sup>1</sup>, Mohamed Mehiri<sup>4</sup>, Marie Dayras<sup>4</sup>, Jacquelin Cassand<sup>4</sup> and Virginia Edgcomb<sup>1,\*,†</sup>

<sup>1</sup>Department of Geology and Geophysics, Woods Hole Oceanographic Institution, 220 McLean, Mail Stop 08, Woods Hole, MA 02543, USA, <sup>2</sup>Laboratoire Universitaire de Biodiversité et Écologie Microbienne, ESIAB, Université de Brest, EA 3882, Technopôle Brest-Iroise, Plouzané, France, <sup>3</sup>Department of Marine Sciences, University of North Carolina Chapel Hill, Chapel Hill, NC, USA and <sup>4</sup>Université Côte d'Azur, CNRS, Institut de Chimie de Nice, UMR 7272, Marine Natural Products Team, 06108 Nice, France

\*Corresponding author: Department of Geology and Geophysics, Woods Hole Oceanographic Institution, 220 McLean, Mail Stop 08, Woods Hole, MA 02543, USA. Tel: +1 508 289 3734; E-mail: vedgcomb@whoi.edu

One sentence summary: Culturable filamentous fungi and yeasts affiliated with Ascomycota and Basidiomycota from Guaymas Basin hydrothermal vent sediments have congeners from other deep-sea habitats and exhibit antibacterial activity against human pathogens.

Editor: Julie Olson

†Virginia Edgcomb, http://orcid.org/0000-0001-6805-381X

# **ABSTRACT**

Relatively little is known about the diversity of fungi in deep-sea, hydrothermal sediments. Less thoroughly explored environments are likely untapped reservoirs of unique biodiversity with the potential to augment our current arsenal of microbial compounds with biomedical and/or industrial applications. In this study, we applied traditional culture-based methods to examine a subset of the morphological and phylogenetic diversity of filamentous fungi and yeasts present in 11 hydrothermally influenced sediment samples collected from eight sites on the seafloor of Guaymas Basin, Mexico. A total of 12 unique isolates affiliating with Ascomycota and Basidiomycota were obtained and taxonomically identified on the basis of morphological features and analyses of marker genes including actin,  $\beta$ -tubulin, small subunit ribosomal DNA (18S rRNA), internal transcribed spacer (ITS) and large subunit ribosomal DNA (26S rRNA) D1/D2 domain sequences (depending on taxon). A total of 11 isolates possess congeners previously detected in, or recovered from, deep-sea environments. A total of seven isolates exhibited antibacterial activity against human bacterial pathogens Staphylococcus aureus ATCC-35556 and/or Escherichia coli ATCC-25922. This first investigation suggests that hydrothermal environments may serve as promising reservoirs of much greater fungal diversity, some of which may produce biomedically useful metabolites.

Keywords: fungal diversity; filamentous fungi; yeasts; hydrothermal vent sediments; antibiotic; antimicrobial activity

## **INTRODUCTION**

The deep sea represents the largest biome on Earth, constituting more than 65% of the Earth's surface and more than 95% of the global biosphere (Herring 2001). Benthic ecosystems in

the deep sea include seamounts, ocean ridges, trenches, abyssal plains, continental slopes and hydrothermal systems where heterotrophic and chemosynthetic microbial communities support deep-sea food webs. Deep-sea fungi were first isolated from

Received: 7 April 2021; Accepted: 8 July 2021

waters 4450 m below the sea surface approximately 50 years ago (Roth, Orpurt and Ahearn 1964) and since then, their biosignatures have been recovered from hadal trenches (e.g. Mariana Trench, Takami et al. 1997), the subsurface sediments of the Canterbury Basin (Rédou et al. 2015), Hydrate Ridge, Eastern Equatorial Pacific, North Pond, Benguela Upwelling System, Peru Margin (Edgcomb et al. 2011; Orsi, Biddle and Edgcomb 2013a; Orsi et al. 2013b) and even the oceanic crust (Li et al. 2020). Additionally, fungi have been cultured from the sediments near the Shimokita Peninsula, Japan (Liu et al. 2016). It has become increasingly clear over the past decade that fungi thrive in the deep sea and influence marine biogeochemical cycles in basaltic ocean crust (Orsi, Biddle and Edgcomb 2013a; Orsi et al. 2013b; Ivarsson et al. 2015a, b), hydrothermal fields (Dekov et al. 2013) and marine sediments (Amend et al. 2010; Bengtson et al. 2014). The concept of a 'mycoloop' suggests that fungi play an essential role in nutrient recycling and thus shape marine and benthic ecosystems (Kagami, Miki and Takimoto 2014). Fungi possess the ability to utilize a wide range of organic substances (Cochrane 1958). Numerous possible carbon sources in marine sediments are available to fungi, including prokaryotic peptidoglycan, lignin, lipids, proteins and amino acids and polysaccharides available in biofilms and necromass. Some of these molecules are considered refractory to biodegradation by most microorganisms (Lee, Wakeham and Arnosti 2004), however, Lomstein et al. (2009) described how fungi use prokaryotic necromass as a carbon source and Orsi, Richards and Francis (2018) reported that fungi in marine sediments secrete exoenzymes that break complex, and often refractory, carbohydrates such as polysaccharides ( $\beta$ -

Current research is decoding the composition of cultured and uncultured fungal communities in marine deep-sea and subsurface sediments. Culture-based investigations of deep-sea sediments have revealed diverse and abundant Ascomycota and Basiodiomycota isolates (Gadanho and Sampaio 2005; Xu, Ou and Wu 2018a; Lai et al. 2007; Burgaud et al. 2009, 2010; Nagano et al. 2010; Singh et al. 2011; Nagahama et al. 2011), have revealed diverse; Singh et al. 2012; Zhang et al. 2014; Xu, Pang and Luo 2014), deep subsurface sediments (Edgcomb et al. 2011; Rédou et al. 2014) and deep-sea chemosynthetic ecosystems, including hydrothermal vents and methane cold seeps (Le Calvez et al. 2009; Rédou et al. 2015; Liu et al. 2016; Xu et al. 2016; Quémener et al. 2020). Molecular investigations of fungi in deep-sea habitats (Bass et al. 2007 phylotypes and novel lineages. For instance, fungal phylotypes and cultured isolates from hydrothermal sites on the East Pacific Rise, Mid-Atlantic Ridge and Lucky Strike (Le Calvez et al. 2009) and from deep-sea methane seeps (Nagahama et al. 2011) include representatives of four of the nine fungal phyla (Opisthosporidia, Chytridiomycota, Ascomycota and Basidiomycota; Naranjo-Ortiz and Gabaldón 2019).

Here, we extend fungal cultivations to hydrothermal and cold seep sediments of Guaymas Basin (Bazylinski, Wirsen and Jannasch 1989). The adjacent Sonora Margin is a cold seep ecosystem with characteristic seep infauna and sulfur-oxidizing microbial mats (Simoneit et al. 1990; GB), a young rift margin system situated in the central Gulf of California, Mexico (Lizarralde et al. 2007). Active hydrothermalism in the southern trough of the GB forms a complex seafloor landscape of sediments with colorful microbial mats and highly variable temperature profiles, hydrothermal edifices, mineral deposits and venting orifices that emit hot fluids (Lonsdale and Becker 1985; Teske et al. 2016). In GB, rapidly deposited organic-rich sediments derived from productive overlying waters and terrigenous

inputs undergo hydrothermal pyrolysis at increased temperature and pressure, which transforms sedimentary organic matter to complex, microbially degradable petroleum compounds (Simoneit and Lonsdale 1982). While hydrothermalism, cold seepage, fluctuating temperatures and the geochemical conditions of GB result in complex and polyextreme microbial habitats, the organic-rich and hydrocarbon-rich sediments also provide potential substrates for fungi.

Studies of GB hydrothermal vent sites have revealed complex and diverse microbial communities of thermophilic Bacteria and Archaea in sediments, fluids and rocks (Amend and Teske 2005; Biddle et al. 2012; McKay et al. 2016).; Dombrowski, Teske and Baker 2018 The initial molecular survey of microbial eukaryote diversity in near-surface hydrothermal sediments of GB revealed fungal SSU rRNA signatures of Ascomycota and Basidiomycota (Edgcomb et al. 2002). Subsequently, it was found that some of these GB phylotypes shared up to 100% sequence similarity with fungal isolates from Mid-Atlantic Ridge hydrothermal sites (Burgaud et al. 2009), indicating widely shared hydrothermal fungal populations.

In this study, we aimed to capture a fraction of in situ fungal diversity using several described media. A complementary aim, knowing that complex microbial communities occur in such habitats with putatively important interactions, was to explore the potential for GB to harbor fungi with abilities to produce antimicrobial compounds. We obtained 12 distinct fungal isolates from the sediments of eight GB on- and off-axis sites, with samples including hydrothermal sediments from the southern Guaymas Basin axial valley (Teske et al. 2016), and off-axis sediments from the northwestern flanks, Octopus Mound, Sonora Margin and Ring Vent locations, as described previously (Teske et al. 2019, 2021; Ramirez et al. 2020). We used these fungal isolates to perform a preliminary assessment of their antibacterial activity against three human bacterial pathogens: Pseudomonas aeruginosa ATCCMP-23 (a Gram-negative multidrugresistant bacterial pathogen), Staphylococcus aureus ATCC-35556 (a Gram-positive bacterial pathogen) and Escherichia coli ATCC-25922 (a Gram-negative bacterial pathogen).

### MATERIALS AND METHODS

# Sample collection

Samples were collected from on- and off-axis sites at the GB during two oceanographic expeditions. Depth of sites ranged from 995 to 2000 m below the sea surface, and sample depths ranged from 0 to 358 cm below seafloor. In October 2014, cold sediments cores of 3-5 m length were collected by piston coring with R/V El Puma (Teske et al. 2019; Ramirez et al. 2020). During R/V Atlantis expedition AT37-06 in December 2016, in situ thermal gradients were measured and push-core samples of hydrothermal seafloor sediments were collected by HOV Alvin (Teske et al. 2021). The sample site locations are shown in Fig. 1. Care was taken to ensure that the in situ temperatures of the sediment samples remained below the highest known temperature limit for fungi (60-62°C, Maheshwari, Bharadwaj and Bhat 2000; Table S1, Supporting Information). Approximately 40 mL of sample material were aliquoted into 50-mL sterile falcon tubes that were overlaid and filled with bottom water before being stored at 4°C until fungal isolations were started ~2 years (R/V El Puma samples) or ~6 months (R/V Atlantis samples) post-collection. Although storage has likely impacted the diversity of recoverable fungi, we used these available live sediments for fungal isolations for

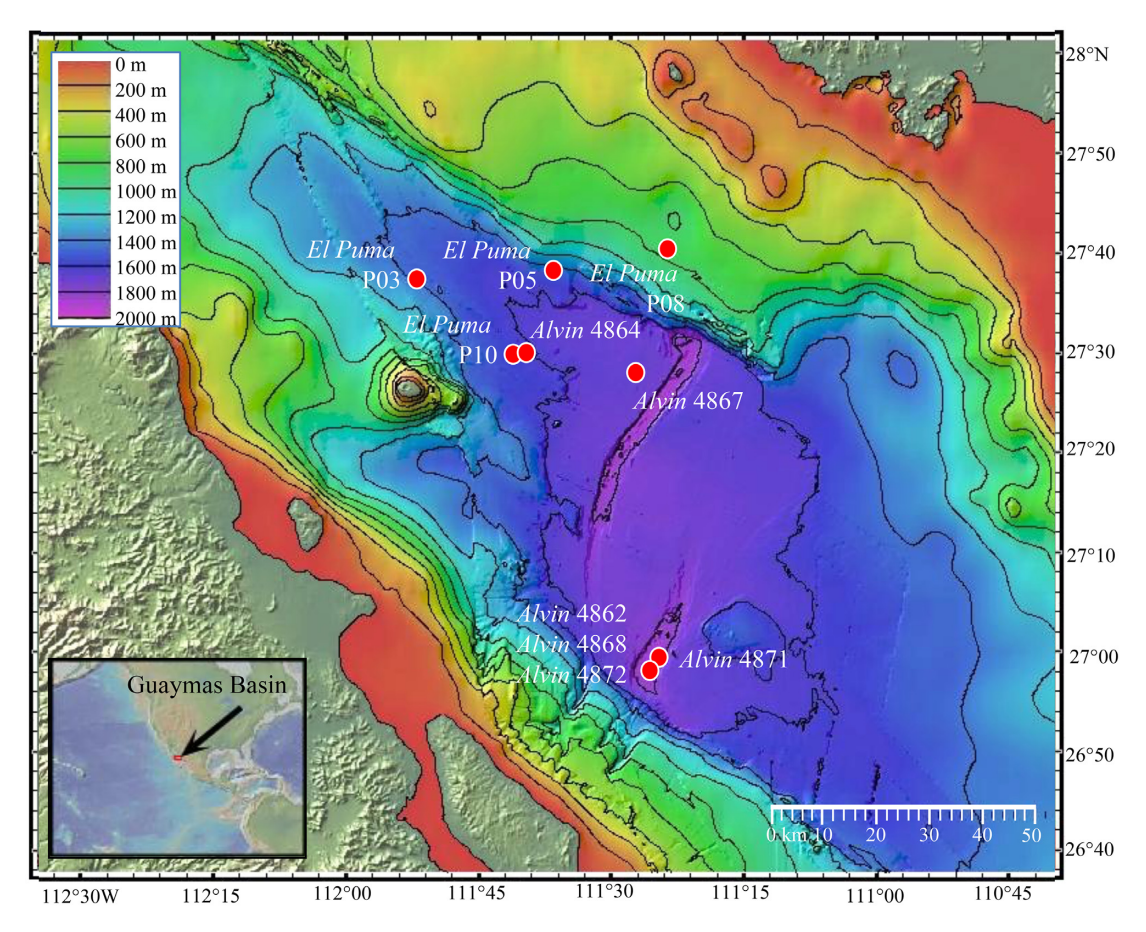


Figure 1. Map of Guaymas Basin denoting the on- and off-axis locations where the eleven sediment samples were collected by research vessels R/V Atlantis and R/V El Puma

these initial explorations of diversity and antimicrobial activity, since the alternative of using frozen (-80°C) sediments from other GB cruises would have implied general freeze-thawing damage to fungal communities. Sample codes for Piston core samples (identified by site and core section number: P03\_4, P05\_3, P08\_3 and P10\_4) and Alvin push cores and samples (identified by dive number and core number, or sample description: 4862-4, 4864 [hydrothermal silicate crusts], 4867-14, 4868-12, 4871-10, 4872-13 and 4872 [weathered hydrocarbon-sediment aggregate]), sampling dates and sites, water depth, in situ temperature and sediment depth are compiled in Table S1 (Supporting Information).

## Sample preparation

Approximately 10 g of each sediment sample were aseptically transferred to sterile 50-mL falcon tubes. Samples containing rock material were crushed in a sterilized stainless-steel mortar and pestle prior to suspension and homogenization. Each sediment subsample was suspended in approximately 25 mL of 1X phosphate buffered saline solution (Thermo Fisher Scientific) and slurries were homogenized using a vortexer at 3000 rpm for 5 min.

## Preparation of enrichment media

To establish initial enrichments, 100  $\mu L$  aliquots of each sediment or rock dilution were spread onto agar plates in triplicate using the following media: Potato Dextrose Agar (PDA, Remel Inc.), Malt Extract Agar (MEA, Sigma Aldrich), Czapek Dox Agar (CDA, Thermo Fisher Scientific), Sabouraud Dextrose Agar (SDA, Oxoid, UK) and Potato Glucose Agar (PGA, Sigma Aldrich). The PDA contained 3.9% potato dextrose agar and 1.2% agar. In some cases, additional agar was added to solidify the media. The MEA contained 3% malt extract agar, 0.5% mycological peptone and 1.5% agar. The CDA contained 3% sucrose, 0.2% sodium nitrate, 0.1% dipotassium phosphate, 0.05% magnesium sulphate, 0.05% potassium chloride, 0.001% ferrous sulphate and 1.5% agar. SDA contained 1% mycological peptone, 4% dextrose and 1.5% agar. PGA contained 3.9% potato glucose agar and 1% agar. All media were prepared with 3% sea salts and with or without the addition of an antibiotic mixture (500 mg/L chloramphenicol, 200 mg/L penicillin G). Hereafter, the presence of antibiotics will be indicated by a '+' after the medium acronym (e.g. MEA+), and the absence of antibiotics will be indicated by a '-' after the medium acronym (e.g. MEA-). All media were autoclaved for 20 min at 121°C and antibiotics were added after the media were cooled to 55-60°C.

### Inoculation of enrichment media

A spiral plater, Bunsen burner and sterile rake were used to spread the sediment slurries over the surface of each plate. All inoculated plates were sealed with Parafilm and incubated aerobically at 23°C under atmospheric pressure (1 atm). This temperature was chosen as a compromise to permit growth of eurythermal fungi that are exposed to cold seafloor temperatures of 3°C in non-hydrothermal GB and Sonora Margin sediments, and to

short-term temperature fluctuations centered around 20-40°C in surficial hydrothermal sediments (McKay et al. 2016). To control for aerial contamination, PDA- and MEA- plates were left exposed on the culture bench during the plate inoculation procedures and during subsequent isolation procedures.

## Culture, isolation and preservation of fungal strains

Fungal colonies (identified as yeasts or filamentous fungi based on macro- and microscopic appearance) that grew on the inoculated plates within a 2-month period were transferred to new plates of the same medium using a sterile inoculation loop. Individual strains with distinct morphology were sub-cultured using a quadrant streak plate method until a pure culture was obtained with a single growth morphology. Growth times between subsequent transfers ranged from several days to several weeks. Filamentous fungi were transferred on PDA- and incubated for 7 days at 23°C to promote sporulation and/or the formation of distinctive structures that could be used to help identify the fungal genus, or to differentiate similar strains. Nonfilamentous fungi were plated on PGA- and incubated for 5 days at 23°C for the same purpose. No fungal colonies were obtained on control plates whose morphology resembled that of fungal isolates in the GB collection, suggesting the absence of aerial and/or anthropogenic laboratory contamination during isolation. The collection of cultured strains was dereplicated prior to molecular identification on the basis of phenotypic analyses (assessment of microscopic and macroscopic characteristics such as growth rate, growth color, texture, colony morphology, cellular appearance under light microscopy (63X and 100X) and medium preference). Selected morphotypes were cryopreserved in Mast Cryobank® (Copan Diagnostics) beads in a glycerol mixture and stored at −80°C.

#### Microscopy

For morphotypes that did not conform to the typical growth pattern of yeasts or filamentous fungi, light and fluorescence microscopy (Zeiss Axio Imager M2 microscope equipped with a Zeiss AxioCam camera, Carl Zeiss Microscopy GmbH) were used at 63X and 100X magnification to visualize the cells and to confirm the presence of chitin. In order to visualize chitin, a drop of lactophenol cotton blue (LPCB) was first deposited on a microscope slide. Fungal cells and aerial hypha were collected using a sterile pipette tip, deposited in the LPCB wet mount, then incubated in the dark for 10 min prior to being observed. Light microscopy under differential interference contrast (DIC) illumination was used for imaging and fluorescence under 4',6diamidino-2-phenylindole (DAPI) illumination was used to confirm the existence of chitin. Spores and branching hyphae were used as indicators of filamentous fungi, whereas budding cells were used to designate yeasts.

#### **DNA** extraction

Prior to the extraction of genomic DNA from each unique morphotype, mycelia (for filamentous fungi) or whole cells (for yeasts) were scraped from the surface of the plates and stored at -20°C. DNA extraction from all fungal cultures was performed following the 2X Lysis/CTAB Extraction Method (Gast, Dennett and Caron 2004) with the modification that the cell pellets were suspended by vortexing for 2 min at 3000 rpm instead of pipetting. The extracted DNAs were stored at  $-20^{\circ}$ C. The quality and quantity of the extracted DNA were confirmed using a NanoDrop (Thermo Fisher Scientific) prior to polymerase chain reaction (PCR) amplification of marker genes for each isolate.

### Amplification of genetic markers

In order to taxonomically affiliate and later dereplicate our isolate collection, several marker genes were PCR-amplified and sequenced for each morphologically unique filamentous fungus and yeast isolate. For filamentous fungi, the internal transcribed spacer (ITS) region of the nuclear ribosomal DNA (nrRNA) gene was amplified using the universal primers ITS1F (5'-CTTGGTCATTTAGAGGAAGTAA) and ITS4 (5'-TCCTCCGCTTATTGATATGC) (White et al. 1990). For the strains affiliated with the genus Penicillium after sequencing of the ITS region, it was necessary to amplify the  $\beta$ -tubulin gene using Bt2a (5'-GGTAACCAAATCGGTGCTGCTTTC) and Bt2b (5'-ACCCTCAGTGTAGTGACCCTTGGC; Glass and Donaldson 1995). For strains related to Cladosporium after ITS region sequencing, the actin gene was amplified using primers ACT-512F (5'-ATGTGCAAGGCCGGTTTCGC) and ACT-783R (5'-TACGAGTCCTTCTGGCCCAT; Carbone and Kohn 1999). For the strains related to the genera Ramularia, Xylaria, Cadophora and Engyodontium on the basis of ITS region sequencing, the 18S ribosomal DNA (rRNA) gene was amplified using primers NS1 (5'-GTAGTCATATGCTTGTCTC) and SR6 (5'-TGTTACGACTTTTACTT; White et al. 1990). For yeasts, the large subunit (26S) rRNA D1/D2 domain was amplified using primers NL1 (5'-GCATATCAATAAGCGGAGGAAAAG) and NL4 (5'-GGTCCGTGTTTCAAGACGG; Gadanho and Sampaio 2005).

All PCRs were performed in 50- $\mu$ L reaction volumes containing 10  $\mu$ L of 5X PCR Buffer, 4  $\mu$ L of MgCl<sub>2</sub> (25 mM), 1  $\mu$ L of each primer (10 mM), 1  $\mu$ L of dNTPs (10 mM), 0.25  $\mu$ L of Taq DNA Polymerase (5U/ $\mu$ L) and 1  $\mu$ L of genomic DNA. The ITS sequence amplification consisted of an initial denaturation step at 95°C for 15 min, followed by 29 cycles of 60 s at 95°C, 60 s at 5°C and 60 s at 72°C, and a final elongation step of 10 min at 72°C. To amplify the large subunit (26S) rRNA D1/D2 domain, an initial denaturation step at 95°C for 15 min was followed by 39 cycles of 60 s at 95°C, 90 s at 52°C and 2 min at 72°C, and a final elongation step of 10 min at 72°C. To amplify  $\beta$ -tubulin genes, an initial denaturation step at 94°C for 15 min was followed by 34 cycles of 60 s at 94°C, 60 s at 61°C and 60 s at 72°C, and a final elongation step of 5 min at 72°C. The actin gene amplification consisted of an initial denaturation step at 95°C for 18 min, followed by 30 cycles of 15 s at 95°C, 20 s at 58°C and 60 s at 72°C, and a final elongation step of 5 min at 72°C. The 18S rRNA gene amplification consisted of an initial denaturation step at 94°C for 15 min, followed by 30 cycles of 45 s at 94°C, 60 s at 44°C and 90 s at 72°C, and a final elongation step of 7 min at 72°C.

The PCR results were visualized on 1% agarose (w/v) gels and photographed under UV transillumination. PCR products were purified (for amplifications producing single bands of the expected size) using 0.7 volume isopropanol, incubated at -20°C for 90 min and centrifuged at 14 000 rpm for 30 min at 4°C. The precipitated DNA pellet was washed with 100  $\mu$ L of 70% ethanol and resuspended in 100  $\mu$ L of sterile H<sub>2</sub>O and DNA quantified using a NanoDrop (Thermo Fisher Scientific). PCR amplicons were Sanger sequenced at GENEWIZ, Inc., Cambridge, MA.

### Phylogenetic analysis

On the basis of gene sequence analysis, the fungal collection was further dereplicated (to eliminate duplicates of genetically similar strains) to 12 isolates. A total of two yeast strains (GB\_4\_Y and

GB\_6\_Y) were found to be morphologically distinct but genetically similar, thus warranting further separate investigation. Taxonomic assignments were initially inferred based on information from one or more genetic markers. We used the Basic Local Alignment Search Tool (BLAST) and the GenBank NCBI non-redundant fungal database (Altschul et al. 1990) to determine the closest genetic relative for each of our isolates (Table 1).

Phylogenetic analyses were used to confirm the identity of each isolate. Sequences of isolates and close relatives (identified using BLASTn) were imported into the MEGA 7.0.26 software (Kumar, Stecher and Tamura 2016) in order to calculate similarities between sequences based on pairwise distances. Sequences were trimmed to equal length prior to ClustalW alignment (Thompson, Higgins and Gibson 1994). Phylogenetic analyses were performed under neighbor-joining criteria with 500 bootstrap replicates in MEGA 7.0.26 using the Maximum Composite Likelihood model. Sequences were considered to be the same species if they were held together by at least 99% bootstrap support under maximum likelihood in analyses of the large subunit (26S) rRNA D1/D2 domain for yeasts, or the ITS sequence for filamentous fungi. Genetic marker sequences are available from GenBank under accession numbers: MT210331-MT210334, MT210324-MT210330, MT247064-MT247068, MT309073, MT310820 and MT364366 (Table 1).

# In vitro antibacterial susceptibility testing

One representative strain from each clade identified in phylogenetic analyses was selected for antibacterial susceptibility testing (AST), and in the case of filamentous fungi, sequencing of additional genetic markers (e.g. actin,  $\beta$ -tubulin and 18S rRNA gene) for identification. On the basis of their phenotypic differences, both GB\_4\_Y and GB\_6\_Y were included despite being assigned to the same species (Aureobasidium pullulans). For selected isolates, one Mast® Cryobank (Copan Diagnostics) cryobead was plated onto the isolate's preferred growth medium using sterile forceps. The plates were incubated at 23°C for 5-7 days to induce regrowth. Each of the 12 unique isolates was transferred to five fresh plates of the same medium to generate sufficient biomass for the AST. The pathogens were grown in Brain Heart Infusion (BHI) broth, which was prepared using 3.7% Bacto® Brain Heart Infusion powder (Becton, Dickinson and Company). Müller Hinton Agar (MHA) plates for the AST were prepared using 3.8% MHA (Sigma Aldrich). Cultures of P. aeruginosa (ATCCMP-23), S. aureus (ATCC-35556) and E. coli (ATCC-25922) were obtained from the American Type Culture Collection (ATCC).

Antibacterial assays (preliminary and confirmatory screenings) were performed using the agar plug diffusion method (Balouiri, Sadiki and Ibnsouda 2016) against the three bacterial strains in order to assess which, if any, of the 12 selected fungal isolates would exhibit inhibitory activity towards any of the three pathogens. For the first round of screening, the fungal isolates were cultured on their previously demonstrated preferred enrichment medium. For fungi that did not exhibit any visible inhibitory activity in the preliminary screening, a different enrichment medium was used in the secondary screening. For example, if an isolate was grown on MEA- initially, it was grown on PDA- for the second round of screening. Similarly, if an isolate was grown on PDA- or PGA- in the first screening, it was grown on MEA- for the second screening. For both screenings, the growth media were prepared without antibiotics.

In preparation for both screenings, each pathogen was grown overnight in BHI broth from glycerol stock cultures stored at -80°C. MHA plates were inoculated with the target bacteria by dispensing 200  $\mu$ L of each bacterial suspension (108 cells/mL) onto the surface of each plate and spreading the suspension with a sterile rake. Plugs from plates of fungal growth (after 72 h growth) were obtained by aseptically using the broad end of a sterile Pasteur pipette. With a sterile needle, the plugs were extracted from the Pasteur pipette and deposited onto the inoculated MHA plates (five plugs per plate, distributed in a quincunx arrangement). The four outer plugs on each plate were placed fungal biomass-down (in direct contact with the bacterial culture), and the fifth plug was placed agar-down in the center of the plate (with the fungal growth not in direct contact with the surface of the plate, only the underlying agar plug). Tests were conducted at the standard temperature for bacterial human pathogens and within the eurythermal range for GB hydrothermal sediments (McKay et al. 2016), at 37°C. Uninoculated media controls were included for MEA, PDA and PGA. The inhibition zones surrounding all plugs were measured at 24, 48 and 72 h in order to quantify antibacterial activity. The radius of each inhibition zone was measured from the center of the fungal plug to the edge of the area cleared of bacterial growth. In the few instances of asymmetrical inhibition zones, we measured the greatest radius, that is, the point at which the distance from the fungal plug to the inhibition zone's edge was maximized.

The presence of a zone of inhibition surrounding each fungal plug indicated antagonistic activity. The radius of the zone was inferred to be proportional to the effectiveness of the antibacterial agent(s) produced by each fungus. For every combination of fungal strain and pathogen, we collected data from 15 plugs in this preliminary screening. When visible clearing zones were observed around plugs, we conducted a second round of confirmatory screening on two additional plates using the same fungal isolate and bacterial pathogen (10 additional fungal plugs tested), yielding a total of 25 plugs (measurements) per experimental combination.

## Secondary metabolites extraction

Freeze-dried fungal biomass was suspended in 50 mL EtOAc: CH<sub>2</sub>Cl<sub>2</sub> mixture (1:1, v/v), homogenized with an ULTRA-TURRAX device (IKA, Wilmington, NC), extracted by sonication and filtered. The process was repeated three times. The combined filtrates were evaporated under reduced pressure to yield a first crude organic extract (F1). The biomass was then suspended in 50 mL MeOH: CH2Cl2 mixture (1:1, v/v), extracted by sonication and filtered. The combined filtrates were evaporated under reduced pressure to yield a second crude organic extract (F2). Crude organic extracts, F1 and F2, were re-suspended in a CH<sub>3</sub>CN: CH<sub>2</sub>Cl<sub>2</sub> mixture (1:1, v/v) and MeOH: CH<sub>2</sub>Cl<sub>2</sub> mixture (1:1, v/v), respectively, to reach a final concentration of 10 mg/mL. Each extract was analyzed by high-performance liquid chromatography (HPLC) combined with both photodiode array and evaporative light scattering detector (ELSD). The latter were performed with a Waters Alliance 2695 HPLC system (Waters Corporation, Milford, MA) coupled with a Waters 996 photodiode array detector and a Sedex 55 evaporative light-scattering detector (SEDERE, France), using a bifunctional Macherey-Nagel NUCLEODUR® Sphinx RP column (250×4.6 mm, 5 μm) consisting of a balanced ration of propylphenyl and C18 ligands. The mobile phase was composed of H<sub>2</sub>O (plus 0.1% HCO<sub>2</sub>H) and acetonitrile (CH3CN plus 0.1% HCO2H) and the following

Table 1. Top BLASTn output for genetic markers of the 12 fungal isolates GB\_1\_FF\_GB\_12\_Y. A bold font in the 'Top BLAST hit' column indicates a consistent identification by our morphological and phylogenetic polyphasic approach. The genus name is followed by 'sp.' for multiple top BLAST hits within the same genus, with identical max scores, total scores, query coverage, e-values and % identities. For top BLAST hits with identical values in different genera, all candidate genera are listed.

Strain ID	Marker gene sequenced, with Genbank number	Top BLAST hit	% identity (%)	e-value
GB_1_FF	ITS region (MT210324)	Cladosporium sp. (MT582794.1)	100	0.0
	Actin gene (MT364366)	Acidomelania paniciola (KF943824.1)	82.91	3e-32
GB_2_FF	ITS region (MT210325)	Penicillium sp. (MT558923.1)	100	0.0
	$\beta$ -tubulin gene (MT309073)	Penicillium chrysogenum (MG832197.1)	99.58	0.0
GB_3_FF	ITS region (MT210326)	Cadophora malorum (KF646089.1)	99.69	0.0
	18S rRNA gene (MT210331)	Rhynchosporium sp., Phialophora sp., Acremonium sp. (KU844336.1, AJ278753.1, AJ278754.1)	100	0.0
GB_4_Y	D1/D2 domain of 26S rRNA (MT247064)	Aureobasidium pullulans, Kabatiella microsticta (MT646038.1, MT107181.1)	100	0.0
GB_5_FF	ITS region (MT210337)	Parengyodontium album (MT610990.1)	100	0.0
	18S rRNA gene (MT210332)	Engyodontium album (AB106650.1)	99.88	0.0
GB <sub>-</sub> 6 <sub>-</sub> Y	D1/D2 domain of 26S rRNA MT247065	Aureobasidium sp., Kabatiella microsticta (MT646038.1, MT107181.1)	100	3e-90
GB_7_Y	D1/D2 domain of 26S rRNA (MT247066)	Torulaspora delbrueckii (MT449110.1)	100	0.0
GB_8_FF	ITS region (MT210328)	Cladosporium parahalotolerans (EF105367.1)	99.83	0.0
	Actin gene (MT310820)	Cadophora sp. (KF646089.1)	99.84	0.0
GB_9_Y	D1/D2 domain of 26S rRNA (MT247067)	Rhodotorula mucilaginosa (MN218618.1)	100	0.0
GB_10_FF	ITS region (MT210329)	Xylaria feejeensis (KR025539.1)	99.67	0.0
	18S rRNA gene (MT210333)	Xylaria sp. (DQ022415.2)	99.87	0.0
GB_11_FF	ITS region (MT210330)	Ramularia eucalypti KJ504798.1)	99.30	0.0
	18S rRNA gene (MT210334)	Zymoseptoria tritici (LT854279.1)	100	0.0
GB_12_Y	D1/D2 domain of 26S rRNA (MT247068)	Dioszegia xingshanensis (KY107649.1)	100	0.0

gradient was used: H<sub>2</sub>O: CH<sub>3</sub>CN 90:10 for 5 min, 90:10 to 0:100 for 30 min, 0:100 for 5 min, 0:100 to 90:10 for 15 min (flow: 1.0 mL/min, injection volume: 20 µL). Chromatograms were extracted at 214, 254 and 280 nm for visual inspection. Moreover, each crude organic extract was analyzed by high-performance liquid chromatography/electrospray ionization tandem mass spectrometry (HPLC/ESI-MS/MS) in both positive and negative ion modes using a Vanquish UHPLC coupled with a Thermo Q-Exactive (Ultra-Performance Liquid Chromatography-High-Resolution Mass Spectrometry (UPLC-HRMS)) Orbitrap (Thermo Fisher Scientific GmbH, Bremen, Germany) spectrometer and an ESI source operated with Xcalibur (version 2.2, ThermoFisher Scientific) software package. A Thermo Scientific Hypersil GOLD column (150×2.1 mm, 3  $\mu$ m) was used with an injection volume of 5 µL and a flow rate of 0.3 mL/min. The mobile phase was composed of H<sub>2</sub>O (plus 0.1% HCO<sub>2</sub>H) and acetonitrile (CH<sub>3</sub>CN plus 0.1% HCO<sub>2</sub>H). The following gradient was used: H<sub>2</sub>O: CH<sub>3</sub>CN 90:10 for 5 min, 90:10 to 0:100 for 30 min, 0:100 for 5 min, 0:100 to 90:10 for 15 min. HR-MS/MS raw data files were converted from .RAW to .mzXML format using the Trans-Proteomic pipeline (Institute for Systems biology, Seattle; Deutsch et al. 2011), and clustered with MS-Cluster using Global Natural Products Social Molecular Networking (GNPS; Wang et al. 2016). A molecular network was created using the online workflow at GNPS. The following settings were used for generation of the network: minimum pairs cos 0.7; parent mass tolerance, 0.02 Da; ion tolerance, 0.02; network topK, 6; minimum matched peaks, 7 and minimum cluster size, 2. Data were visualized and analyzed using Cytoscape 3.6.0.

#### **RESULTS**

## Fungal isolations from environmental samples

Culturing efforts using the 11 sediment samples as starting inoculum on several types of media initially yielded  $\sim$ 30 fungal isolates. The final 12 distinct isolates showed macro- and microscopic morphologies (Fig. 2) that were broadly categorized as single-celled yeasts or filamentous fungi, identified by 'Y' or 'FF' strain designations, respectively. Due to their phenotypic plasticity, fungi grown on different enrichment media (e.g. PDA(+/-), MEA(+/-), PGA(+/-)) often produce colonies with different phenotypic characteristics (Islam and Ohga 2013). For this reason, we dereplicated the culture collection on the basis of marker gene sequences. Unique isolates comprised two genera within the phylum Basidiomycota (GB\_9\_Y, Rhodotorula and GB\_12\_Y, Dioszegia), and eight genera within the phylum Ascomycota (GB\_1\_FF, Cladosporium; GB\_2\_FF, Penicillium; GB\_3\_FF and GB\_8\_FF, Cadophora; GB\_4\_Y and GB\_6\_Y, Aureobasidium; GB\_5\_FF, Engyodontium; GB\_7\_Y, Torulaspora; GB\_10\_FF and Xylaria; GB\_11\_FF, Ramularia). As shown by Genbank BLASTn comparisons, 11 of the 12 isolates possess close cultured relatives from other deep-sea habitats (Table 3).

## Phylogenetic analyses

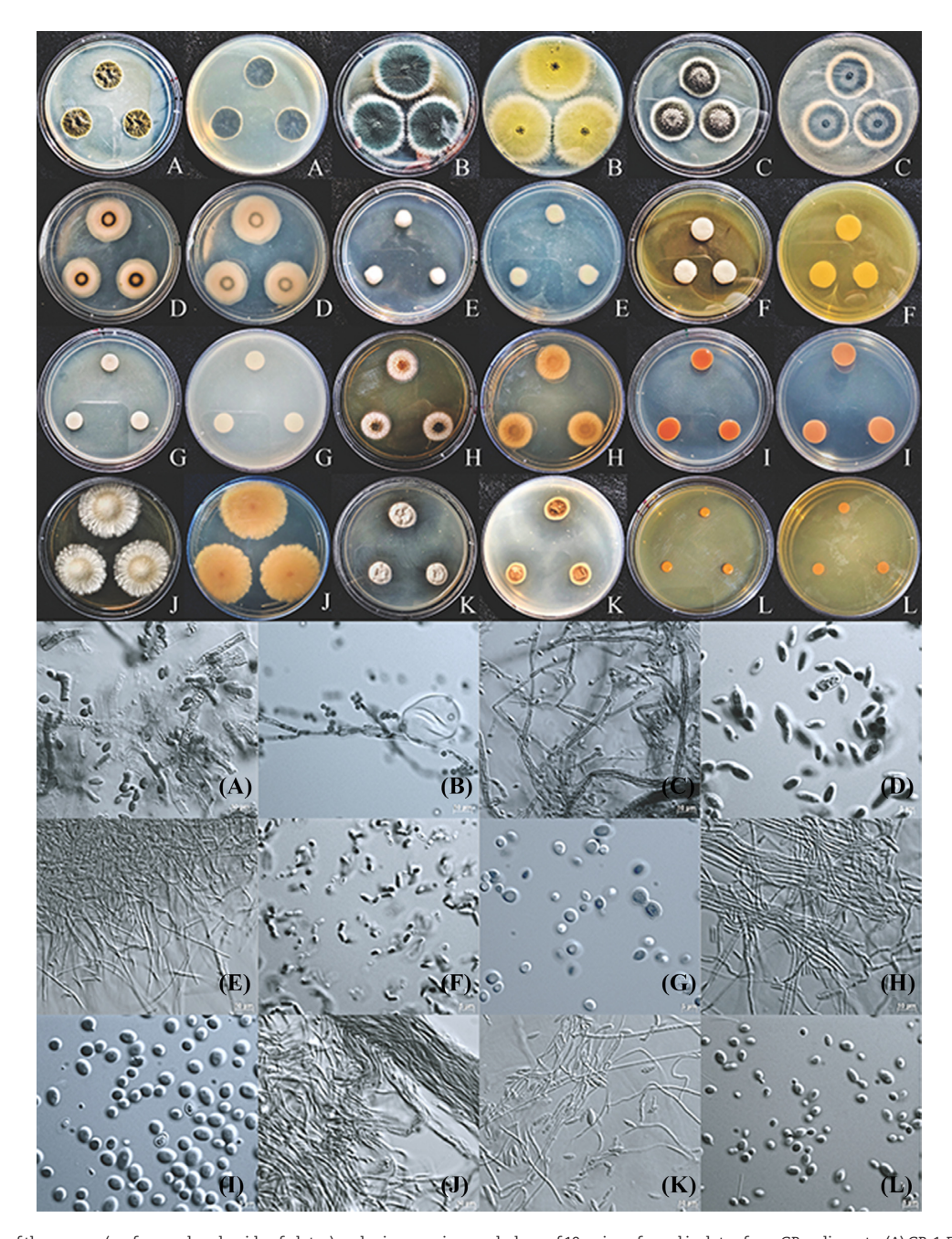
Phylogenetic analyses of morphologically distinct yeast strains (based on the D1/D2 domain of the large subunit (26S) rRNA gene) revealed they were affiliated with taxa within four genetically distinct clusters (Fig. 3). GB\_9\_Y grouped with Rhodotorula strains by 87% maximum likelihood bootstrap support. GB\_12\_Y was affiliated with Dioszegia xingshanensis with 100% bootstrap support. The clustered but morphologically different strains

Table 3. Geographic occurrences of the congeners to GB fungal isolates GB\_1.FF-GB\_12.FF, listed with sampling location, latitude/longitude coordinates, water and subseafloor depths and literature reference. GB\_7.Y does not currently have a documented congener from a marine sampling site.

		Site information	nation					Filamentous congeners	congeners			Yes	Yeast congeners	s
				-qnS										
Site category	Sampling location short description	Latitude and longitude, in decimal minutes	Water depth [m]	seafloor depth [mbsf]	Literature Reference	Clado- sporium GB_1_FF	Peni- cillium GB_2.FF	Cado- phora GB_3_FF	Engyo- dontium GB_5_FF	Xylaria GB_10_FF	Ramularia GB_111_FF	basidium GB-4-Y GB-6-Y	Rhodo- torula GB_9_Y	Dioszegia GB_12_Y
Deep sub-surface	IODP Site U1352, Canterbury Basin, New Zealand sediments	44°56.2662 S 172°01.3630 E	344	4-1884	Rédou et al. (2015)	×	×					×	×	
	IODP site G0020A, Shimokita Peninsula, Japan, sediments	41°10.5983 N 142°12.0328 E	1180	1289–2457	Liu et al. (2017)	×	×							
	IODP Site 1473A, Atlantis Bank, Gabbro Massif rock, Indian Ocean	32°42.3622 S 57°16.6880 E	710	750	Quemener et al. (2020)						×			
Deep ocean water and seafloor	South China Sea deep-sea sediments	17°59.742 to 20°22.971 N; 111°48.092 to 120°00.250 E	2326– 3928	Surface	Zhang et al. (2013)	×	×			×		×		
	South China Sea deep-sea sediment	19° 00.368 N, 117° 58.223 E	3739	Surface	Yao et al. (2014)				×					
	East Indian Ocean deep-sea sediments	2°57'S to 10°00'N; 84°33' to 95°19'E	4530– 4810	Surface	Zhang et al. (2014)	×	×					×		
	East Pacific deep-sea sediments	07°37′ N, 145°02′ W	5115	Surface	Yan et al. (2009)			×						
	Ierapetra Basin and Harodotus Abussal	34°30.308 to	2689-	Surface	Imhoff	×	×		×			×		
	plain sediments, Mediterranean	25°58.554 to 36°33.065 E	000		Sevastou et al. (2020)									
	Yap hadal trench	138°20 to 137°52 E; 8°02 to 8°05N	4159 -6682	Surface	Gao et al. (2020)	×	×		×				×	
	Yap Trench cold	11°46.303 N	3702 and	Surface	Monday								×	
	sedineins, and Iheya Rise hydrothermal	27°27.240 N 126°53.892 E	100		Hamamoto and									
	sediments				Horikoshi (2006)									
Seep habitats	Sao Paulo plateau asphalt seep sediments	20°43.1448 S 38°38.1529 W, 20°41.1448 S 38°38.1529 W	2651 and 2720	Surface	Nagano et al. (2017); Jiang et al. (2018)		×	×						
	Methane-oxidizing Lamellibrachia tubeworms, Sagami Bay, Japan	35°00'N 139°14'E	1156	Surface	Nagahama et al. (2001)								×	

Table 3. Continued

		Site information	nation					Filamentous congeners	; congeners			Yes	Yeast congeners	S
				-qns		7		7	) F					
	Sampling location	Latitude and longitude, in	Water	seatloor depth	Literature	Clado- sporium	Penı- cillium	Cado- phora	Engyo- dontium	Xylaria	Ramularia	basıdıum GB.4.Y	Knodo- torula	Dioszegia
Site category	short description	decimal minutes	depth [m]	[mbsf]	Reference	GB_1_FF	GB_2_FF	GB.3.FF	GB_5_FF	GB_10_FF	GB_11_FF	GB_6_Y	GB_9_Y	GB.12_Y
Hydro-thermal habitat	Southwest Indian Ridge calcareous ooze, volcanic debris	47°25′ to 52°59′ E, and 35°54′ to 38°47′ S	1879– 2699	Surface	Xu et al. (2018)	×	×						×	
	South Mid-Atlantic Ridge hydrothermal chimney fragments	13°35′ W, 15°16′ S	2770	Surface	Xu et al. (2017)	×	×							
	Kueishan Island hydrothermal sediments (Taiwan)	24°83′ N, 122°00′ E	10 to 80	Surface	Pang et al. (2019)	×	×			×				
	Western Pacific hydrothermal sediments	126°53.898 E, 27°47.25 N	1028	Surface	Han et al. (2020)		×							
	Mid-Atlantic hydrothermal shrimp Rimicaris exoculata (Rainbow vent field)	36°08' N, 34°00' W	2300	Surface	Rédou et al. (2016)			×						
	Rainbow vent field Black smoker rocks	36°08 N, 34°00 W	2300	Surface	Burgaud et al. (2009)							×	×	
	Mid-Atlantic Mount Saldanha	36°35.251 N, 33°26.685 W	2116	Surface	Gadanho et al. (2005)								×	
	Fe-oxidizing mats and basalt exposure at Nafanua crater, Vailulu'u seamount	14°12.889 S, 707 ar 168°03.568W 14'13.062 1667 S, 169°06.114 W	707 and 062 1667	Surface	Connell et al. (2009)								×	×



 $\textbf{Figure 2.} \ Images of the macro-(surface and underside of plates) and microscopic morphology of 12 unique fungal isolates from GB sediments. (A) GB\_1\_FF/Cladosporium for the macro-(surface and underside of plates) and microscopic morphology of 12 unique fungal isolates from GB sediments. (A) GB\_1\_FF/Cladosporium for the macro-(surface and underside of plates) and microscopic morphology of 12 unique fungal isolates from GB sediments. (A) GB\_1\_FF/Cladosporium for the macro-(surface and underside of plates) and microscopic morphology of 12 unique fungal isolates from GB sediments. (A) GB\_1\_FF/Cladosporium for the macro-(surface and underside of plates) and microscopic morphology of 12 unique fungal isolates from GB sediments. (A) GB\_1\_FF/Cladosporium for the macro-(surface and underside of plates) and microscopic morphology of 12 unique fungal isolates from GB sediments. (A) GB\_1\_FF/Cladosporium for the macro-(surface and underside of plates) and microscopic morphology of 12 unique fungal isolates for the macro-(surface and underside of plates) and microscopic morphology of 12 unique fungal isolates for the macro-(surface and underside of plates) and microscopic morphology of 12 unique fungal isolates for the macro-(surface and underside of plates) and microscopic morphology of 12 unique fungal isolates for the microscopic morphology of 12 unique fungal isolates for the microscopic morphology of 12 unique fungal isolates for the microscopic morphology of 12 unique fungal isolates for the microscopic morphology of 12 unique fungal isolates for the microscopic morphology of 12 unique fungal isolates fun$ sp., (B) GB.2.FF/Penicillium chrysogenum, (C) GB.3.FF/Cadophora sp., (D) GB.4.Y/Aureobasidium pullulans, (E) GB.5.FF/Engyodontium album, (F) GB.6.Y/Aureobasidium pullulans, (E) GB.5.FF/Engyodontium album, (E) GB.6.Y/Aureobasidium pullulans, (E) GB.5.FF/Engyodontium album, (E) GB.6.Y/Aureobasidium pullulans, (E) GB.5.FF/Engyodontium album, (E) GB.6.Y/Aureobasidium pullulans, (E) GB.6.Y/Au lulans, (G) GB.7.Y/Torulaspora delbrueckii, (H) GB.8.FF/Cadophora sp., (I) GB.9.Y/Rhodotorula mucilaginosa, GB.10.FF/Xylaria feejeensis, GB.11.FF/Ramularia eucalypti and GB\_12\_Y/Dioszegia xingshanensis. The magnification used to acquire the microscopic images was 63X.

GB\_4\_Y and GB\_6\_Y were affiliated with Aureobasidium pullulans with 100% bootstrap support. GB\_7\_Y was affiliated with Torulaspora delbrueckii with 97% bootstrap support. Analysis of the D1/D2 domain of the 26S rRNA gene showed that GB\_4\_Y, GB\_6\_Y, GB\_7\_Y, GB\_9\_Y and GB\_12\_Y shared 100% sequence identity with A. pullulans, T. delbrueckii, Rhodotorula mucilaginosa and D. xingshanensis, respectively (Table 1).

Filamentous fungal isolates were identified using a polyphasic approach merging morphological and phylogenetic analyses. Taxonomic identification based on phylogeny of ITS sequences (Fig. 4) was supplemented by information from additional genetic markers, including actin,  $\beta$ -tubulin and 18S rRNA gene sequences for selected filamentous isolates (Table 1). These analyses revealed seven genetically unique strains. GB\_1\_FF was affiliated to Cladosporium strains, GB\_2\_FF was affiliated to Penicillium strains, and GB\_3\_FF was affiliated to strains Cadophora and Philalocephala strains, with 100% bootstrap support each (Fig. 4). GB\_5\_FF was affiliated with a strain in the genus Engyodontium with >99% bootstrap support. GB\_8\_FF was affiliated with Cladosporium strains with 92% bootstrap support based on ITS sequence, but its morphology and actin gene sequence placed this isolate into the genus Cadophora (see below). GB\_10\_FF

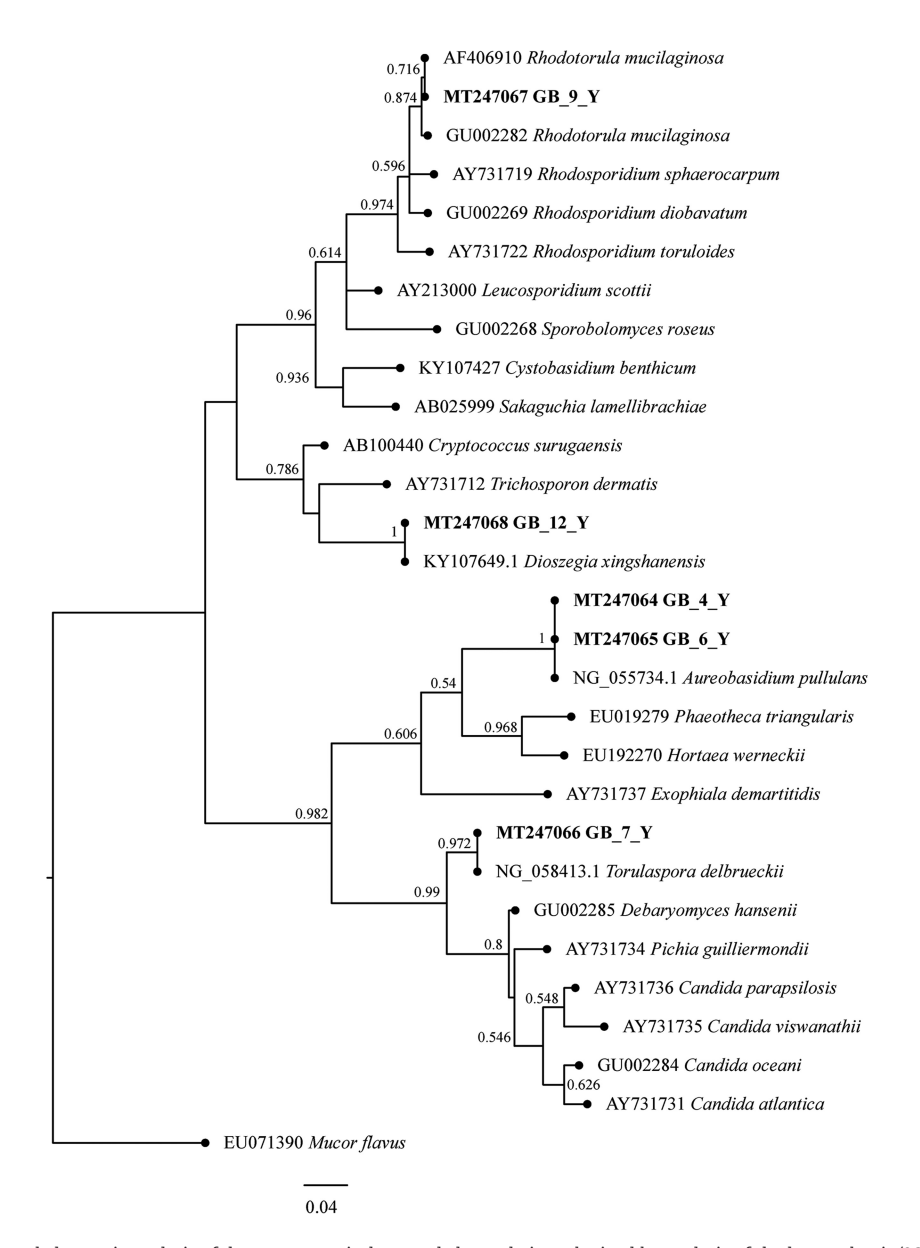


Figure 3. Neighbor joining phylogenetic analysis of deep-sea yeast isolates and close relatives obtained by analysis of the large subunit (26S) rRNA D1/D2 domain sequences bootstrapped 500 times using MEGA7. Bootstrap values >0.5 are shown. Mucor flavus (EU071390) belonging to the Mucoromycota phylum was used as outgroup. All sequences are listed with their GenBank accession numbers.

was affiliated with a strain in the genus Xylaria with 100% bootstrap support. Finally, GB\_11\_FF was affiliated with several Ramularia strains with 62-100% bootstrap support.

Strains GB\_1\_FF, GB\_3\_FF and GB\_8\_FF were further identified to the genus level based on complementary macro- and microscopical observations. GB\_1\_FF was confirmed as a Cladosporium based on its suede-like olivaceous-brown colonies with dematiaceous hyphae and smooth conidia with a distinct dark hilum. GB\_3\_FF and GB\_8\_FF were confirmed as Cadophora spp. based on colony characteristics (flat, felty, cottony in the middle and with an edge and varying colors from brown/golden in the center to white) and the branched, septate hyphae, with hyphal swellings and phialides producing ovoid to elongated conidia (Fig. 2).

## Antibacterial screening results

Of the final 12 isolates, seven exhibited some degree of inhibitory activity (clearing of bacterial growth on plates under or surrounding agar plugs that supplied fungal growth) against at least one of the three target pathogens tested (Table 2). Of those seven isolates, all inhibited the growth of S. aureus (GB\_1\_FF, GB\_2\_FF, GB\_4\_Y, GB\_7\_Y, GB\_8\_FF, GB\_10\_FF and GB\_11\_FF), and showed average inhibition zone radii of 15.9±2.7 mm, 6.5±5.2 mm, 5.3±3.8 mm, 18.2±2.7 mm, 18.3±2.6 mm, 10.9±5.4 mm 15.7±3.9 mm after 72h, respectively (Fig. 5). Aside GB\_4\_Y, these strains also inhibited growth of E. coli, with average inhibition radii of  $1.9\pm3.2$  mm,  $1.3\pm3.0$  mm,  $10.4\pm1.6$  mm,  $7.5\pm1.6$  mm,  $3.1\pm3.6$  mm and 7.7±3.3 mm after 72 h, respectively (Fig. 5). None of the 12 fungal isolates produced a visible zone of inhibition against P. aeruginosa. Bacterial colonies interspersed within the inhibition zones

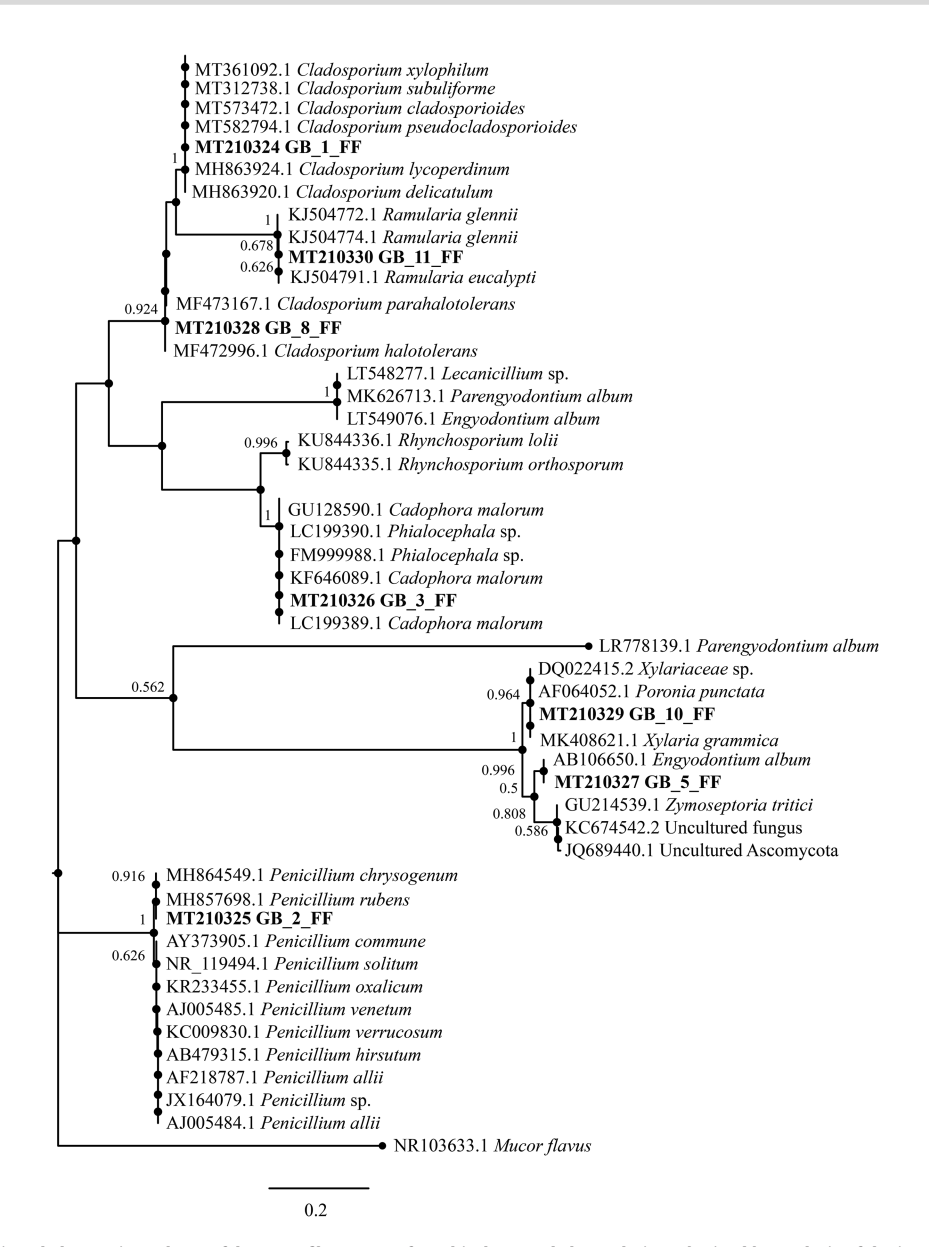


Figure 4. Neighbor joining phylogenetic analyses of deep-sea filamentous fungal isolates and close relatives obtained by analysis of the internal transcribed spacer (ITS) region sequences bootstrapped 500 times using MEGA7. Bootstrap values > 0.5 are shown. Mucor flavus (EU071390) belonging to the Mucoromycota phylum was used as outgroup. Note GB.8.FF morphology and its actin gene sequence place it within Cadophora. All sequences are listed with their GenBank accession numbers.

were observed in some instances. The yeast isolates GB\_4\_Y and GB\_7\_Y, both assigned to A. pullulans, showed intraspecific variability; GB\_4\_Y inhibited S. aureus and GB\_7\_Y inhibited both S. aureus and E. coli. Similarly, the Cadophora strains GB\_3\_FF and GB\_8\_FF exhibited distinct inhibitory activity towards these test pathogens despite belonging to the same genus. In our assays, GB\_8\_FF inhibited the growth of both S. aureus and E. coli, while GB\_3\_FF demonstrated no measurable antagonistic activity toward either pathogen.

The seven fungi that demonstrated inhibitory activities against the pathogenic targets on specific media (GB\_1\_FF, GB\_2\_FF, GB\_4\_Y, GB\_7\_Y, GB\_8\_FF, GB\_10\_FF and GB\_11\_FF) were selected for secondary metabolite extraction.

Metabolomic fingerprints associated with each organic extract were obtained by HPLC-PDA-ELSD and UHPLC-HRESIMS. This permitted the characterization of the chemical diversity of the extracts, including the number, relative amounts, chemical

family and molecular mass of the constitutive metabolites. Our fungal strains, with the exception of GB\_2\_FF, produced very few secondary metabolites (Fig. 7).

MS/MS data associated with each metabolite within each extract were referenced against the ones available in databases (MarinLit, Dictionary of Natural Products, Scifinder and Chemspider) and the published data (Uchida et al. 1996; Kusano et al. 1997; Komai et al. 2005; Liu, Sutton and Sternglanz 2005; Du et al. 2010; Yunianto et al. 2014; Dekan et al. 2019; Wang et al. 2019a). The main compound produced by Penicillium sp. (GB.2.FF) was assigned to meleagrin along with some other known compounds (e.g. andrastins A and C, austalide X, bilaid A, penisimplicin B, roquefortines (C, F or I), simplicissin and tetrahydrotrichodimerol; Fig. 8). In using the same approach, we assigned the major metabolite produced by the fungus Xylaria feejeensis (GB\_10\_FF) to 3R-(+)-5-0-[6'-0-acetyl]- $\alpha$ -D-glucopyranosyl-5-hydroxymellein (Wang et al. 2019b). Finally,

Table 2. Summary of inhibitory activity of all twelve unique fungal isolates against Staphylococcus aureus and Escherichia coli at 24, 48 and 72 h. The use of bolded font for the average inhibition zone radius indicates complete inhibition zones, likewise, the use of non-bolded font indicates incomplete inhibition zones. The use of bolded font for the culture medium indicates the medium that was used when inhibition occurred (relevant for the instances where two media types are listed). Values are mean  $\pm$  SD (mm; n = 25).

Fungal strain ID	Culture medium	Bacterial taxa screened against	Average inhibition zone radius at 24 h (mm)	Average inhibition zone radius at 48 h (mm)	Average inhibition zone radius at 72 h (mm)
GB_1_FF	PDA-	S. aureus ATCC-35556	16.1±2.4	16.4±2.2	14.0±3.9
		E. coli ATCC-25922	1.1±2.2	1.6±3.0	4.5±4.4
GB_2_FF	PDA-/MEA-	S. aureus ATCC-35556	$7.0 \pm 5.0$	5.6±4.8	$7.3 \pm 5.7$
		E. coli ATCC-25922	1.7±2.8	1.0±2.6	1.4±3.4
GB_3_FF	PDA-/MEA-	S. aureus ATCC-35556 E. coli ATCC-25922	-	-	-
GB_4_Y	PGA-/ <b>MEA-</b>	E. con ATCC-25922 S. aureus ATCC-35556	6.1±4.1	4.6±3.5	5.2±4.1
		E. coli ATCC-25922			
GB_5_FF	PGA-/MEA-	S. aureus ATCC-35556	-	-	-
		E. coli ATCC-25922			
GB_6_Y	MEA-/PDA-	S. aureus ATCC-35556 E. coli ATCC-25922	-	-	-
GB_7_Y	PDA-	S. aureus ATCC-35556	17.9±2.9	19.3±1.8	16.5±3.4
		E. coli ATCC-25922	10.0±2.3	10.9±0.9	10.0±0.0
GB_8_FF	MEA-	S. aureus ATCC-35556 E. coli ATCC-25922	17.6±2.8 <b>6.2±0.8</b>	18.8±2.5 <b>8.4±1.5</b>	18.5±2.4 <b>8.3±1.5</b>
GB_9_Y	PDA-/MEA-	S. aureus ATCC-35556 E. coli ATCC-25922	-	-	-
GB_10_FF	MEA-	S. aureus ATCC-35556	10.0±3.9	9.7±5.9	16.0±3.9
		E. coli ATCC-25922	2.4±3.4	2.6±3.7	6.0±2.5
GB_11_FF	PDA-	S. aureus ATCC-35556	15.8±3.0	16.5±4.3	13.5±4.1
		E. coli ATCC-25922	8.6±3.7	7.7±2.5	5.3±3.4
GB_12_Y	MEA-/PDA-	S. aureus ATCC-3556 E. coli ATCC-25922	-	-	-

Cladosporium lycopodium (GB\_1\_FF) and T. delbrueckii (GB\_7\_Y) produce one compound each with m/z values of 331.2262 ([M+H]+) and 277.1137 ([M+H]+), respectively (not listed in databases; Fig. 8A).

The graphical representation of the molecular network of GB\_2\_FF strain using MS/MS data of the crude organic extracts F1 (red) and F2 (blue) allowed to highlight 1710 nodes and 1956 edges that suggest a production of numerous metabolites (Fig. 8B). The subcluster of the main compound, meleagrin, contains 29 nodes and 63 edges. Thus, the presence of different compounds in the same cluster underlines a common biosynthetic pathway and some metabolites appearing as analogues of meleagrin (Fig. 8).

## DISCUSSION

#### Methodological considerations

The cultivation results have to be interpreted cautiously by recognizing fundamental constraints that limited the diversity of isolates obtained. First, the cultivations were not performed at in situ hydrostatic pressure (~200 atm), nor were they conducted at site-specific temperatures. Second, aerobic cultivation conditions were employed. While anaerobic conditions commonly exist in organic-rich marine sediments below the sediment surface, periodic availability of oxygen in porewaters can be provided through subsurface fluid flows, particularly in relatively dynamic hydrothermal settings. Nonetheless, aerobic cultivation conditions undoubtedly restricted recovered fungal diversity. Third, sediment samples were overlaid with bottom water in sealed sterilized jars that were stored at 4°C for long periods prior to their use as inoculum in this study. Not all in situ microorganisms will survive those conditions. Finally, limited culturing approaches (including diversity of media types) recover only a fraction of viable in situ microbiota, as shown by environmental marker gene sequencing surveys of fungi in deep-sea sediments that detected taxa that remain uncultured to this day (Le Calvez et al. 2009). The consistently observed occurrence pattern of the fungi we recovered in diverse deepsea marine sediments (Table 3) indicates that these strains meet the recent updated definition of marine fungi (Pang et al. 2016) and are thus genuinely marine-adapted taxa, as detailed in the following section.

## Fungal diversity and occurrence patterns

To our knowledge, this is the first report of cultured fungal isolates from GB hydrothermal sediments, and the first exploration of their antimicrobial activities. Our findings suggest that among the congeners of the Guaymas Basin isolates, Cladosporium and Penicillium species (congeners of GB\_1\_FF and GB\_2\_FF) appear to be ubiquitous in benthic and subseafloor habitats of different depths. Worldwide, the most reported genera of filamentous fungi are Penicillium, Aspergillus, Aureobasidium, Cladosporium, Trichoderma, Alternaria, Acremonium, Fusarium, Hortaea and Exophiala; while the most reported genera of yeast form are Rhodotorula, Candida, Malassezia, Cryptococcus, Pichia, Rhodosporidium and Trichosporon (Vargas-Gastélum and Riquelme 2020). Penicillium is one of three genera, along with Aspergillus and Candida, that are particularly abundant in marine habitats (Balabanova et al. 2018). Its wide distribution in terrestrial (McRae, Hocking

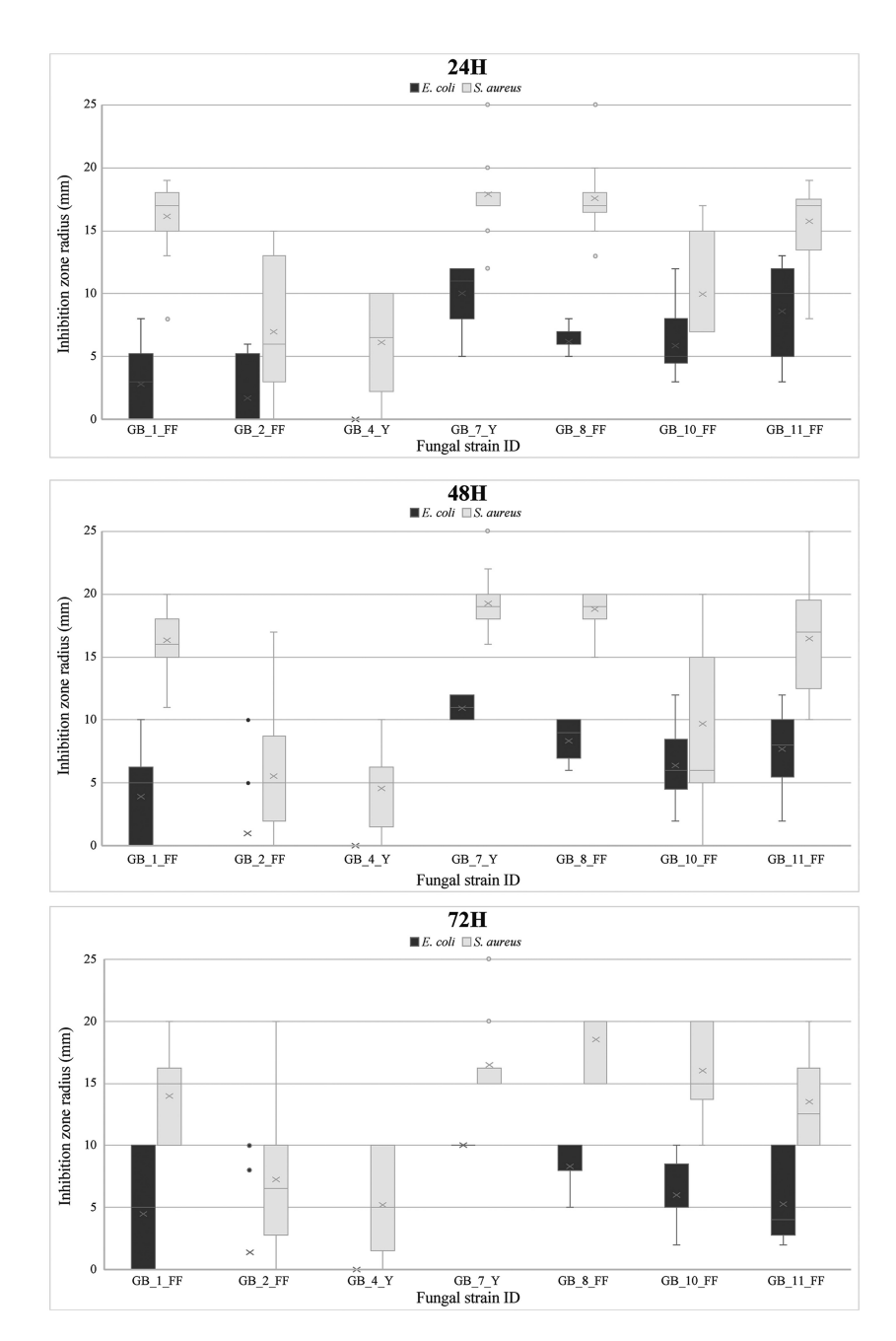


Figure 5. Relative inhibitory activity (radius of inhibition zone (mm)) of seven fungal isolates that inhibited Staphylococcus aureus and/or Escherichia coli at 24, 48 and 72 h. Values are mean  $\pm$  SD (mm; n = 25).

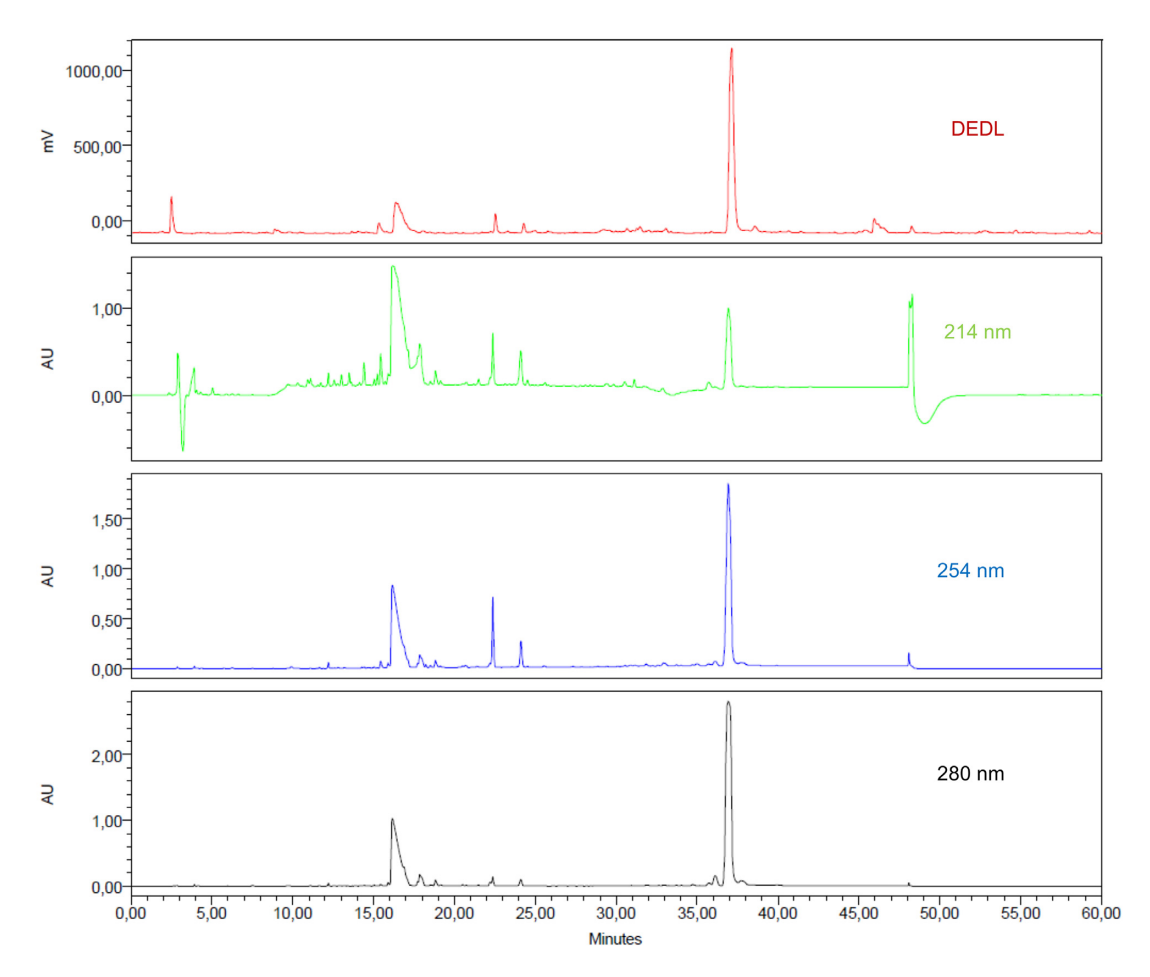
and Seppelt 1999) and freshwater ecosystems (Heo et al. 2019) suggests high adaptability. Among the Cadophora congeners of GB\_3\_FF, the Mid-Atlantic Ridge strain Cadophora malorum Mo12 strain was characterized as a halophilic psychrotrophic fungus (Burgaud et al. 2009), and some Cadophora isolates from Antarctic environments were described as psychrotrophs (Duncan 2007).

All of our yeast isolates, with the exception of Torulaspora isolate GB\_7\_Y, possess congeners previously isolated from deepsea habitats (Table 3). Among these, A. pullulans is widespread in different marine habitats, including hypersaline waters in marine solar salterns (Gunde-Cimerman and Zalar 2014), polar habitats (Zalar and Gunde-Cimerman 2014), the terrestrial phyllosphere (Grube, Schmid and Berg 2011) and food (Samson,

Hoekstra and Frisvad 2004). Due to this versatility, A. pullulans is often defined as polyextremotolerant.

# Preliminary assessment of antibacterial activities of fungal isolates

Fungal functions in the deep biosphere have been linked to cell-cell competition based on evidence for synthesis of antimicrobial secondary metabolites revealed by metatranscriptomic (Pachiadaki et al. 2016) and culture-based approaches (Rédou et al. 2015; Svahn et al. 2012; Navarri et al. 2016). Thus, bioprospecting for microorganisms and metabolites in less-studied untapped habitats, such as deep-sea sediments and hydrothermal systems, might yield new results in the search for novel



 $\textbf{Figure 7}. \ \ \textbf{Metabolomic fingerprints of GB.2.FF dichloromethane-ethyl acetate extract obtained with HPLC-PDA-ELSD (Macherey-Nagel NUCLEODUR @ Sphinx RP column of the property of the$  $(250\times4.6 \text{ mm},\ 5\ \mu\text{m}),\ gradient:\ H_2O\ plus\ 0.1\%\ HCO_2H:\ CH_3CN\ plus\ 0.1\%\ HCO_2H,\ 90:10\ for\ 5\ min,\ 90:10\ to\ 0:100\ for\ 30\ min,\ 0:100\ for\ 5\ min,\ 0:100\ to\ 90:10\ for\ 15\ min).$ 

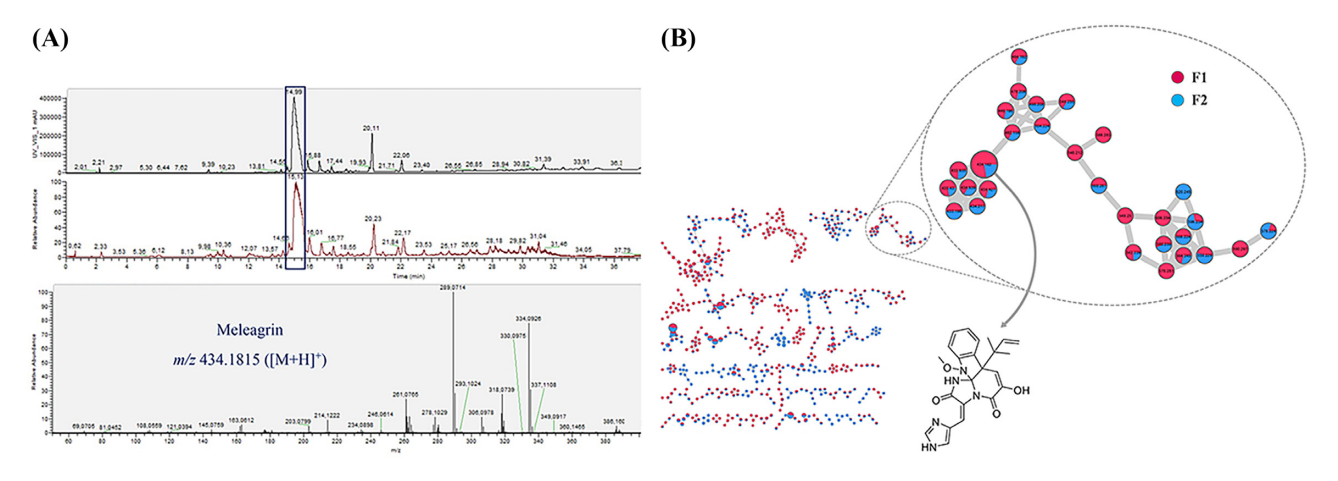


Figure 8. (A) HPLC-HR-ESI (+) analyses of the GB.2.FF dichloromethane-ethyl acetate extract and MS/MS spectrum of meleagrin (Hypersil GOLD, 150 × 2.1 mm; 5  $\mu$ m, gradient: CH3CN + 0.1% formic acid (FA), H2O + 0.1% FA, 10:90 to 100:0 in 30 min). (B) Molecular network built using MS/MS data from the crude organic extracts F1 (red) and F2 (blue) of GB.2.FF strain. The subcluster of the main compound meleagrin of GB.2.FF is highlighted.

antibiotics. Over the past 50 years, over 30 000 natural products (NPs) have been discovered from marine samples, approximately 2% of which were synthesized by deep-sea microorganisms (Skropeta and Wei 2014). Filamentous fungi in particular have yielded diverse clinically relevant natural products (Rateb and Ebel 2011; Blunt et al. 2018), including approximately 20% of all existing antibiotics (Demain 2014). In 1953, the first

marine-derived antibiotic, cephalosporin C, was isolated from an Acremonium species collected from the Sardinian coast (Abraham et al. 1953). A total of 25 years later, the antimicrobial gliotoxin was isolated from a deep-sea strain of Aspergillus sp. (Ascomycota) from marine sediments of Japan (Okutani 1977). The first antibiotic derived from a marine yeast was Indanonaftol A, a spiro-indanone derivative from a marine Aureobasidium sp. with weak activity against Gram-positive bacteria (Biabani and Laatsch 2004).

According to a review by Arifeen et al. (2020), 151 bioactive compounds have been extracted from deep sea-derived fungi in the last 5 years. A number of antibiotic compounds (e.g. Methylisoverrucosidinol, Penicillisocoumarin A-D, Aspergillumarins B, Dehydroaustin, Dehydroaustinol, 7-hydroxydehydroaustin, Austinone, Austinol, Austin, Austinolide and Pestalotionol; and Ascomycotin A, Diorcinol, Lindgomycin, Ascosetin and Canescenin A and B) have been isolated from hydrothermal vent- and deep-sea sediment-derived fungi (Arifeen et al. 2020).

In our exploration of antimicrobial activity against the human pathogens P. aeruginosa, S. aureus, or E. coli, the strongest inhibitory activity was demonstrated by GB\_4\_Y (A. pullulans) against S. aureus. A. pullulans has known biotechnological importance due to its ability to produce the following compounds: pullulan, a linear glucan with numerous applications in food, pharmaceutical and biomedical fields (Singh, Kaur and Kennedy 2019); liamocins, with activity on cancer cell lines and weak bacterial activity against Enterococcus faecalis (Bischoff et al. 2015); and the antifungal antibiotics Aureobasidin A to R (Takesako et al. 1991). Some investigations into the antimicrobial activity of different strains of Aureobasidium reported activities against both Gram-negative and -positive bacteria (McCormack, Wildman and Jeffries 1994), while others reporting activity against Gram-negative bacteria but not against Gram-positive bacteria (Kalantar, Deopurkar and Kapadnis 2006). Altogether, intraspecific variability seems to play a significant role and requires screening numerous strains from untapped habitats.

The six other fungal isolates that inhibited both S. aureus and E. coli showed a greater effect on S. aureus. For instance, Cadophora strain GB\_8\_FF showed an average inhibition zone of 18.3±2.6 mm and 7.5±1.6 mm against S. aureus and E. coli, respectively (over 72 h). Cadophora sp. have been found throughout the world in diverse terrestrial and marine habitats (Almeida et al. 2010; Rusman et al. 2015; Yakti, Kovács and Franken 2019), yet they remain rarely studied in the context of the production of putatively interesting secondary metabolites. Interestingly, the genome of a deep-sea hydrothermal vent Cadophora malorum strain contained numerous genes encoding biotechnologically relevant enzymes and genes involved in the synthesis of secondary metabolites (Rédou et al. 2016). Our study reinforces the potential utility of isolates affiliated to the genus Cadophora.

Interpretations of our data on inhibition zone radii for any combination we tested must be made with caution, however, because in spite of efforts to be consistent, we could not accurately quantify the amount of fungal growth transferred with each test agar plug. This undoubtedly contributed to observed variation in sizes of zones of inhibition for individual plugs on a single plate (Fig. 6). On all plates, we took a single, radial measurement of each zone of inhibition. When asymmetrical inhibition zones were encountered, we measured the maximum radius. This may have over-estimated the inhibitory activity around those agar plugs, however asymmetrical zones were infrequent, and measuring 25 replicates (i.e. plugs) per test helped to minimize the effects of any over-estimates and outliers. Additionally, the use of 37°C as the incubation temperature in our antibacterial assays likely affected fungal metabolite production and therefore should be explored in the future.

For each fungus-pathogen test, one centrally located agar plug was placed with the agar surface in direct contact with the surface of the test plate (fungal biomass on plug facing away from plate surface). This central plug was surrounded by four plugs that were all placed with fungal biomass in direct contact with the test pathogen. This allowed us to examine if metabolites diffused into the agar plug would elicit a stronger response. GB\_2\_FF (tested against E. coli and S. aureus), GB\_7\_Y (tested against S. aureus) and GB\_10\_FF (tested against E. coli) exhibited the most potent inhibitory activity when the plug was placed in this agar-down configuration, suggesting that inhibitory agent(s) had been produced prior to exposure to the pathogen (Fig. 4 panels (C), (D), (J) and (M)) and did not require direct contact between the pathogen and fungus. Although fungal cell walls can display polysaccharides (with potentially cytotoxic properties), as previously demonstrated for terrestrial (Giavasis 2014) and some marine (e.g. Sun et al. 2016; Chen et al. 2016; Li et al. 2016) fungi, the antibacterial agent(s) produced by these taxa appear to be secreted extracellularly.

Of the inhibition zones observed in this study (over the course of 72 h), 54% were complete and 46% were incomplete. Complete inhibition zones (e.g. Fig. 6 panel (G)) were produced by GB\_1\_FF (tested against E. coli), GB\_2\_FF (tested against E. coli), GB\_7\_Y (tested against E. coli), GB\_7\_Y (tested against S. aureus), GB\_8\_FF (tested against E. coli), GB\_10\_FF (tested against E. coli) and GB\_11\_FF (tested against E. coli). The complete zones of inhibition suggest the synthesis of bactericidal metabolites that kill bacterial cells. The presence of incomplete inhibition zones (e.g. Fig. 6 panel (I)) populated by sparsely distributed colonies surrounding the fungal plugs suggests these fungi produce bacteriostatic compounds that bacteria can more easily circumvent through genetic mutations or metabolic 'workarounds' (Salyers and Whitt 2005). Colonies growing within zones of inhibition are unlikely to represent anthropogenic contamination since their morphology was consistent with that of the pathogen. Where present, the number of colonies appearing within these zones did not vary noticeably between 24 and 72 h.

#### Secondary metabolites

The metabolites produced by GB\_2\_FF have previously been isolated from fungi belonging to the Penicillium genus. Some of the annotated metabolites (e.g. Andrastin C, Penisimplicin B and Simplicissin) have only been isolated from terrestrial fungi (Uchida et al. 1996; Kusano et al. 1997; Komai et al. 2005). Thus, this is the first time that these compounds have been identified from fungi isolated from the marine environment. Concerning the biological activities of the annotated compounds, the compound meleagrin does not exhibit antimicrobial activities with the disk diffusion method (Yunianto et al. 2014). The antibiofilm activity of meleagrin was investigated against Gram-positive (S. aureus ATCC 29213) and Gram-negative (P. aeruginosa ATCC 9027) bacteria, and found to have a minimum inhibitory concentration (MIC) of 0.25 mg/mL and 0.6 mg/mL, respectively (Hamed et al. 2020). Meleagrin shows moderate cytotoxicity against cancer cell lines (Du et al. 2010), and its biosynthetic precursor roquefortine C is a relatively common fungal metabolite that inhibits growth of Gram-positive bacteria (Kopp and Rehm 1981); both Roquefortines and tetrahydrotrichodimerol showed cytotoxicity against cancer cells lines (Liu, Sutton and Sternglanz 2005; Du et al. 2009; Du et al. 2010). Andrastin A exhibits no antibacterial activity on Bacillus cereus and Streptococcus faecalis (Trinh 2017) and Andrastin C has not be evaluated for antimicrobial activities but is known to be a protein farnesyltransferase inhibitor (Uchida et al. 1996). Finally, Penisimplicin exhibited no antifungal activities and the other compounds have



Figure 6. Images of representative inhibition zones for each test combination (fungus vs. pathogen) that yielded a zone of inhibition. (A) G.1.FF vs. E. coli, (B) GB.1.FF vs. S. aureus, (C) GB.2.FF vs. E. coli, (D) GB.2.FF vs. S. aureus, (E) GB.4.Y vs. S. aureus, (F) GB.7.Y vs. E. coli, (G) GB.7.Y vs. S. aureus, (H) GB.8.FF vs. E. coli, (I) aureus, (J) GB.10.FF vs. E. coli, (K) GB.10.FF vs. S. aureus, (L) GB.11.FF vs. E. coli, (M) GB.11.FF vs. S. aureus, (N) E. coli control plate and (O) S. aureus control plate.

never been evaluated for their antimicrobial activities (Austalide X, Simplicissin). For the fungus Xylaria feejeensis (GB\_10\_FF), a candidate secondary metabolite (3R-(+)-5-O-[6'-O-acetyl]- $\alpha$ -D-glucopyranosyl-5-hydroxymellein) has already been isolated from Xylaria spp., but never evaluated for its biological properties (Wang et al. 2014). Many fungal isocoumarin derivatives are known for their antibacterial and antifungal activities (Noor et al. 2020). Therefore, the isolation and evaluation of antimicrobial properties of this annotated compound is necessary in the future. The molecular networking approach used here allows to highlight numerous unassigned compounds and their derivatives for which complementary analyses are needed. Similarly, the unknown metabolites from GB\_1\_FF and GB\_7\_Y could be isolated and characterized to evaluate their biological properties.

## **OUTLOOK**

Identifying metabolites of interest synthesized by these fungi requires more extensive testing to elucidate the chemical structure of metabolites produced, their properties (including potential toxicity to humans), novelty and activity against a broader selection of pathogens. Future studies could expand on these results by investigating additional pathogens, strain-level variations in antimicrobial activity and metabolites produced, and the effects of incubation temperatures and pressures as well as media types (nutrient sources) on antimicrobial activity and metabolite production. The number of unique isolates can undoubtedly also be expanded by utilizing a wider range of media and redox conditions, allowing longer incubation times during initial enrichments from deep-sea samples, and utilizing freshly collected material. Hydrothermal sites and sediments such as those at the GB may be promising sources of fungi with potential medical and biotechnological applications.

### **AUTHOR CONTRIBUTIONS**

AT collected samples. EK, GB and VE conceived the experimental design. EK and VE conducted all experiments. GB performed phylogenetic analyses. MM, MD and JC contributed metabolomic data. All authors contributed to manuscript preparation.

## **ACKNOWLEDGMENTS**

We thank the Alvin and Sentry teams for their tremendous support during Guaymas Basin cruise AT37-06 and targeted sampling of hydrothermal sediments during Alvin dives. We thank the Science crew of R/V El Puma for excellent piston coring skills and a very enjoyable sediment sampling cruise. Finally, the authors would like to thank Maxence Quemener (U. Brest, France) for generating the phylogenetic trees presented in the paper.

## **SUPPLEMENTARY DATA**

Supplementary data are available at FEMSRE online.

#### **FUNDING**

E. Keeler's work was supported by NSF Biological Oceanography grant 1829903 to V. Edgcomb, the Marjot Foundation and the Kurt Giessler Foundation. Sampling for this project was funded by collaborative NSF Biological Oceanography grants 1357238 and 1357360 to A. Teske and S.B. Joye, respectively. Current Guaymas Basin research in the Teske lab is supported by NSF Biological Oceanography grant 1829680. Piston core sampling in Guaymas Basin was funded by NSF OCE grant 1449604 to A. Teske. M. Dayras is the recipient of a thesis grant from the 'Conseil Régional Provence Alpes Côte d'azur'. This work has been supported by the French government, through the UCAJEDI Investments in the Future project managed by the National Research

Agency (ANR) with the reference number ANR-15-IDEX-01. We thank the Canceropôle Provence-Alpes-Côte d'Azur, and the Provence-Alpes-Côte d'Azur Region for the financial support provided to the MetaboCell project.

Conflicts of interest. None declared.

### REFERENCES

- Abraham EP, Newton GG, Crawford K et al. Cephalosporin N: a new type of penicillin. Nature 1953;171:343.
- Almeida C, Eguereva E, Kehraus S et al. Hydroxylated sclerosporin derivatives from the marine-derived fungus Cadophora malorum. J Nat Prod 2010;73:476-8.
- Altschul SF, Gish W, Miller W et al. Basic local alignment search tool. J Mol Biol 1990;215:403-10.
- Amend A, Burgaud G, Cunliffe M et al. Fungi in the marine environment: open questions and unsolved problems. mBio 2010;10. DOI: 10.1128/mBio.01189-18.
- Amend JP, Teske A. Expanding frontiers in deep subsurface microbiology. Palaeogeogr Palaeoclimatol Palaeoecol 2005; **219**:131-55.
- Arifeen MZ, Ma Y, Xue Y et al. Deep-sea fungi could be the new arsenal for bioactive molecules. Mar Drugs 2020;19:9.
- Balabanova L, Slepchenko L, Son O et al. Biotechnology potential of marine fungi degrading plant and algae polymeric substrates. Front Microbiol 2018;9:1527.
- Balouiri M, Sadiki M, Ibnsouda SK. Methods for in vitro evaluating antimicrobial activity: a review. J Pharmaceut Anal 2016:6:71-9.
- Bass D, Howe A, Brown N et al. Yeast forms dominate fungal diversity in the deep oceans. Proc R Soc 2007;274:3069-77.
- Bazylinski DA, Wirsen CO, Jannasch HW. Microbial utilization of naturally occurring hydrocarbons at the Guaymas Basin hydrothermal vent site. Appl Environ Microbiol 1989;55:2832-
- Bengtson S, Ivarsson M, Astolfo A et al. Deep-biosphere consortium of fungi and prokaryotes in Eocene subseafloor basalts. Geobiology 2014; 12:489-96.
- Biabani MA, Laatsch H. Advances in chemical studies on lowmolecular weight metabolites of marine fungi. Adv Synth Catal 2004;340:579-607.
- Biddle JF, Cardman Z, Mendlovitz H et al. Anaerobic oxidation of methane at different temperature regimes in Guaymas Basin hydrothermal sediments. ISME J 2012;6:1018-31.
- Bischoff KM, Leathers TD, Price NP et al. Liamocin oil from Aureobasidium pullulans has antibacterial activity with specificity for species of Streptococcus. J Antibiot (Tokyo) 2015;68:642-45.
- Blunt JW, Carroll AR, Copp BR et al. Marine natural products. Nat Prod Rep 2018;35:8-53.
- Bode HB, Bethe B, Höfs R et al. Big effects from small changes: possible ways to explore nature's chemical diversity. Chem-BioChem 2002;3:619-27.
- Burgaud G, Arzur D, Durand L et al. Marine culturable yeasts in deep-sea hydrothermal vents: species richness and association with fauna. FEMS Microbiol Ecol 2010;73:121-33.
- Burgaud G, Le Calvez T, Arzur D et al. Diversity of culturable marine filamentous fungi from deep-sea hydrothermal vents. Environ Microbiol 2009;11:1588-600.
- Carbone I, Kohn LM. A method for designing primer sets for speciation studies in filamentous ascomycetes. Mycologia 1999;91:553-56.

- Chen Y, Mao WJ, Yan MX et al. Purification, chemical characterization, and bioactivity of an extracellular polysaccharide produced by the marine sponge endogenous fungus Alternaria. Mar Biotechnol 2016;18:301-13.
- Cochrane VW. Physiology of fungi. New York: John Wiley & Sons,
- Connell LB, Barrett AW, Templeton A et al. Fungal diversity associated with an active deep sea volcano: vailulu'u Seamount, Samoa. Geomicrobiol J 2009;26:597-605.
- Dekan Z, Sianati S, Yousuf A et al. A tetrapeptide class of biased analgesics from an Australian fungus targets the  $\mu$ -opioid receptor. Proc Natl Acad Sci 2019 116:22353-58.
- Dekov VM, Bindi L, Burgaud G et al. Inorganic and biogenic Assulfide precipitation at seafloor hydrothermal fields. Mar Geol 2013; **342**:28–38.
- Demain AL. Importance of microbial natural products and the need to revitalize their discovery. J Ind Microbiol Biotechnol 2014;41:185-201.
- Deutsch EW, Mendoza L, Shteynberg D et al. A guided tour of the trans-proteomic pipeline. Proteomics 2011;10:1150-59.
- Dick GJ. The microbiomes of deep-sea hydrothermal vents: distributed globally, shaped locally. Nat Rev Microbiol 2019;17:271-83.
- Dombrowski N, Teske AP, Baker BJ. Expansive microbial metabolic versatility and biodiversity in dynamic Guaymas Basin hydrothermal sediments. Nat Commun 9, 2018. DOI: 10.1038/s41467-018-07418-0.
- Du L, Feng T, Zhao B et al. Alkaloids from a deep ocean sedimentderived fungus Penicillium sp. and their antitumor activities. J Antibiot (Tokyo) 2010;63:165-70.
- Du L, Li DH, Zhu TJ et al. New alkaloids and diterpenes from a deep ocean sediment derived fungus Penicillium sp. Tetrahedron 2009;65:1033-39.
- Duncan SM. Fungal diversity and cellulytic activity in the Historic Huts, Ross Island, Antarctica (Thesis, Doctor of Philosophy (PhD)) 2007. The University of Waikato, Hamilton, New Zealand.
- Edgcomb VP, Beaudoin D, Gast R et al. Marine subsurface eukaryotes: the fungal majority. Environ Microbiol 2011;13:172-83.
- Edgcomb VP, Kysela DT, Teske A et al. Benthic eukaryotic diversity in the Guaymas Basin hydrothermal vent environment. Proc Natl Acad Sci 2002;99:7658-62.
- Gadanho M, Sampaio JP. Occurrence and diversity of yeasts in the mid-Atlantic ridge hydrothermal fields near the Azores Archipelago. Microb Ecol 2005;50:408-17.
- Gao Y, Du X, Xu W et al. Fungal diversity in deep sea sediments from East Yap Trench and their denitrification potential. Geomicrobiol J 2020;37:848-58.
- Gast RJ, Dennett MR, Caron DA. Characterization of protistan assemblages in the Ross Sea, Antarctica, by denaturing gradient gel electrophoresis. Appl Environ Microbiol 2004;70:2028-
- Giavasis I. Bioactive fungal polysaccharides as potential functional ingredients in food and nutraceuticals. Curr Opin Biotechnol 2014;26:162-73.
- Glass NL, Donaldson GC. Development of primer sets designed for use with the PCR to amplify conserved genes from filamentous ascomycetes. Appl Environ Microbiol 1995;61:1323-
- Grube M, Schmid F, Berg G. Black fungi and associated bacterial communities in the phyllosphere of grapevine. Fung Biol 2011;115:978-86.
- Gunde-Cimerman N, Zalar P. Extremely halotolerant and halophilic fungi inhabit brine in solar salterns around the globe. Food Technol Biotechnol 2014;52:170-79.

- Hamed A, Abdel-Razek A, Araby M et al. Meleagrin from marine fungus Emericella dentata Nq45: crystal structure and diverse biological activity studies. Nat Prod Res 2020;19:1-9.
- Han W, Cai J, Zhong W et al. Protein tyrosine phosphatase 1B (PTP1B) inhibitors from the deep-sea fungus Penicillium chrysogenum SCSIO 07007. Bioorg Chem 2020;96. DOI: 10.1016/j.bioorg.2020.103646.
- Heo I, Hong K, Yang H et al. Diversity of Aspergillus, Penicillium, and Talaromyces species isolated from freshwater environments in Korea. Mycobiology 2019;47:12-9.
- Herring P. The biology of the deep ocean. Oxford: Oxford University Press, 2001.
- Imhoff JF. Natural products from marine fungi still an underrepresented resource. Marine Drugs 2016;14:19.
- Islam F, Ohga S. Effects of media formulation on the growth and morphology Ectomycorrhizae and their association with host plant. ISRN Agronomy 2013;2013:1-12.
- Ivarsson M, Bengtson S, Skogby H et al. A fungal-prokaryotic consortium at the basalt-zeolite interface in subseafloor igneous crust. PLoS ONE 2015a;10:e0140106.
- Ivarsson M, Broman C, Gustafsson H et al. Biogenic Mn-Oxides in subseafloor basalts. PLoS ONE 2015b;10:e0128863.
- Jiang K, Zhang J, Sakatoku A et al. Discovery and biogeochemistry of asphalt seeps in the North São Paulo Plateau, Brazilian Margin. Sci Rep 2018. 8. DOI: 10.1038/s41598-018-30928-2.
- Kagami M, Miki T, Takimoto G. Mycoloop: chytrids in aquatic food webs. Front Microbiol 5, 2014. DOI: 10.3389/fmicb.2014.00166.
- Kalantar E, Deopurkar R, Kapadnis B. Antimicrobial activity of indigenous strains of Aureobasidium isolated from Santalum album leaves. Iran J Pharm Res 2006; 5:59-64.
- Kohlmeyer J, Kohlmeyer E. Marine mycology: the higher fungi. New York: Academic Press, 1979.
- Komai S, Hosoe T, Itabashi T et al. Two new meroterpenoids, penisimplicin A and B, isolated from Penicillium simplicissimum. Chem Pharm Bull 2005;53:1114-7.
- Kopp B, Rehm HJ. Studies on the inhibition of bacterial macromolecule synthesis by roquefortine, a mycotoxin from Penicillium roqueforti. App Microbiol 1981;13:232-35.
- Kumar S, Stecher G, Tamura K. MEGA7: molecular evolutionary genetics analysis version 7.0 for bigger datasets. Mol Biol Evol 2016;33:1870-74.
- Kusano M, Koshino H, Uzawa J et al. Simplicissin, a new pollen growth inhibitor produced by the fungus, Penicillium cf. simplidssimum (Oudemeans) Thorn No. 410. Biosci Biotechnol Biochem 1997;61:2153-55.
- Lai X, Cao L, Tan H et al. Fungal communities from methane hydrate-bearing deep-sea marine sediments in South China Sea. ISME J 2007;1:756-62.
- Le Calvez T, Burgaud G, Mahé S et al. Fungal diversity in deep-sea hydrothermal ecosystems. Appl Environ Microbiol 2009;75:6415-21.
- Lee C, Wakeham S, Arnosti C. Particulate organic matter in the sea: the composition conundrum. AMBIO J Hum Environ 2004;33:565-75.
- Leersnyder ID, Gelder LD, Driessche IV et al. Influence of growth media components on the antibacterial effect of silver ions on Bacillus subtilis in a liquid growth medium. Sci Rep 2018;8. DOI: 10.1038/s41598-018-27540-9.
- Li H, Chi Z, Wang X et al. Purification and characterization of extracellular amylase from the marine yeast Aureobasidium pullulans N13d and its raw potato starch digestion. Enzyme Microb Technol 2007;40:1002-12.

- Li H, Gao T, Wang J et al. Structural identification and antitumor activity of the extracellular polysaccharide from Aspergillus terreus. Process Biochem 2016;51:1714-20.
- Li J, Mara P, Schubotz F et al. Recycling and metabolic flexibility dictate life in the lower oceanic crust. Nature 2020;579:250-5.
- Liu C, Huang X, Xie T et al. Exploration of cultivable fungal communities in deep coal-bearing sediments from  $\sim$ 1.3 to 2.5 km below the ocean floor. Environ Microbiol 2016;19:803-18.
- Liu B, Sutton A, Sternglanz R. A yeast polyamine acetyltransferase. J Biol Chem 2005; 280:16659-64.
- Lizarralde D, Axen G, Brown H et al. Variation in styles of rifting in the Gulf of California. Nature 2007;448:466-69.
- Lomstein A, Niggemann J, Jorgensen B et al. Accumulation of prokaryotic remains during organic matter diagenesis in surface sediments off Peru. Limnol Oceanogr 2009;54:1139-51.
- Lonsdale P, Becker K. Hydrothermal plumes, hot springs, and conductive heat flow in the Southern Trough of Guaymas Basin. Earth Planet Sci Lett 1985;73:211-25.
- McCormack PJ, Wildman HG, Jeffries P. Production of antibacterial compounds by phylloplane-inhabiting yeasts and yeastlike fungi. Appl Environ Microbiol 1994;60:927-31.
- McKay L, Klokman VW, Mendlovitz HP et al. Thermal and geochemical influences on microbial biogeography in the hydrothermal sediments of Guaymas Basin, Gulf of California. Environ Microbiol Rep 2016;8:150-61.
- McRae CF, Hocking AD, Seppelt RD. Penicillium species from terrestrial habitats in the Windmill Islands, East Antarctica, including a new species, Penicillium antarcticum. Pol Biol 1999;**21**:91-111.
- Maheshwari R, Bharadwaj G, Bhat MK. Thermophilic fungi: their physiology and enzymes. Microbiol Mol Biol Rev 2000;64:461-
- Nagahama T, Hamamoto M, Horikoshi K. Rhodotorula pacifica sp. nov., a novel yeast species from sediment collected on the deep-sea floor of the north-west Pacific Ocean. Int J Syst Evol Microbiol 2006;56:295-99.
- Nagahama T, Hamamoto M, Nakase T et al. Distribution and identification of red yeasts in deep-sea environments around the northwest Pacific Ocean. Antonie Van Leeuwenhoek 2001;80:101-10.
- Nagahama T, Takahasi E, Nagano Y et al. Molecular evidence that deep-branching fungi are major fungal components in deep-sea methane cold-seep sediments. Environ Microbiol 2011;13:2359-70.
- Nagano Y, Miura T, Nishi S et al. Fungal diversity in deep-sea sediments associated with asphalt seeps at the Sao Paulo Plateau. Deep Sea Res Part II 2017;146:59-67.
- Nagano Y, Nagahama T, Hatada Y et al. Fungal diversity in deepsea sediments - the presence of novel fungal groups. Fung Ecol 2010;3:316-25.
- Naranjo-Ortiz MA, Gabaldón T. Fungal evolution: diversity, taxonomy and phylogeny of the Fungi. Biol Rev 2019;94:2101-37.
- Navarri M, Jégou C, Meslet-Cladière L et al. Deep subseafloor fungi as an untapped reservoir of amphipathic antimicrobial compounds. Mar Drugs 2016;14:50.
- Noor AO, Almasri DM, Bagalagel AA et al. Naturally occurring isocoumarins derivatives from endophytic fungi: sources, isolation, structural characterization, biosynthesis, and biological activities. Molecules 2020;25:395.
- Okutani K. Gliotoxin Produced by a strain of Aspergillus isolated from marine mud. J-Stage 1977:43;995-1000.
- Orsi W, Biddle JF, Edgcomb V. Deep sequencing of subseafloor eukaryotic rRNA reveals active fungi across marine subsurface provinces. PLoS ONE 2013a;8:e56335.

- Orsi WD, Edgcomb VP, Christman GD et al. Gene expression in the deep biosphere. *Nature* 2013b;499:205–08.
- Orsi WD, Richards TA, Francis WR. Predicted microbial secretomes and their target substrates in marine sediment. *Nat Microbiol* 2018;**3**:32–7.
- Pachiadaki MG, Rédou V, Beaudoin DJ et al. Fungal and prokaryotic activities in the marine subsurface biosphere at Peru Margin and Canterbury Basin inferred from RNA-based analyses and microscopy. Front Microbiol 2016;7. DOI: 10.3389/fmicb.2016.00846.
- Pang K, Guo S, Chen I et al. Insights into fungal diversity of a shallow-water hydrothermal vent field at Kueishan Island, Taiwan by culture-based and metabarcoding analyses. PLoS ONE 2019;14:e0226616.
- Pang KL, Overy DP, Gareth Jones EB et al. 'Marine fungi' and 'marine- derived fungi' in natural product chemistry research: toward a new consensual definition. Fung Biol Rev 2016;30:163–75.
- Quémener M, Mara P, Schubotz F et al. Meta-omics highlights the diversity, activity and adaptations of fungi in deep oceanic crust. SfAM 2020;22:3950–67.
- Ramirez GA, McKay LJ, Fields MW et al. The Guaymas Basin Subseafloor Archaeome reflects complex environmental histories. iScience 2020 23:101459.
- Rateb ME, Ebel R. Secondary metabolites of fungi from marine habitats. Nat Prod Rep 2011;28:290–344.
- Rédou V, Ciobanu M, Pachiadaki M et al. In-depth analyses of deep subsurface sediments using 454-pyrosequencing reveals a reservoir of buried fungal communities at recordbreaking depths. FEMS Microbiol Ecol 2014;90:908–21.
- Rédou V, Kumar A, Hainaut M et al. Draft genome sequence of the deep-sea ascomycetous filamentous fungus Cadophora malorum Mo12 from the Mid-Atlantic Ridge reveals its biotechnological potential. Genome Announc 2016;4:467–516.
- Rédou V, Navarri M, Meslet-Cladière L et al. Species richness and adaptation of marine fungi from deep-subseafloor sediments. Appl Environ Microbiol 2015;81:3571–83.
- Richards TA, Jones MDM, Leonard G et al. Marine fungi: their ecology and molecular diversity. Ann Rev Mar Sci 2012;4:495–522.
- Roth FJ, Orpurt PA, Ahearn DG. Occurrence and distribution of fungi in a subtropical marine environment. *Can J Bot* 1964;42:375–83.
- Rusman Y, Held BW, Blanchette RA et al. Soudanones A–G: antifungal isochromanones from the ascomycetous fungus Cadophora sp. isolated from an iron mine. J Nat Prod 2015;78:1456–60.
- Salyers AA, Whitt DD. Revenge of the microbes: How bacterial resistance is undermining the antibiotic miracle. Washington, D.C: ASM Press, 2005.
- Samson RA, Hoekstra ES, Frisvad JC. Introduction to food-and airborne fungi. Utrecht: Utrecht: Centraalbureau voor Schimmelcultures 2004
- Sevastou KN, Lampadariou D, Mouriki A et al. Meiofaunal distribution in the Levantine Basin (Eastern Mediterranean): spatial variability at different scales, depths and distance-to-coast. Deep Sea Res Part II 2020;171:104635.
- Simoneit BRT, Lonsdale PF. Hydrothermal petroleum in mineralized mounds at the seabed of Guaymas Basin. *Nature* 1982;295:198–202.
- Simoneit BRT, Lonsdale PF, Edmond JM et al. Deep-water hydrocarbon seeps in Guaymas Basin, Gulf of California. Appl Geochem 1990;5:41–9.

- Singh P, Raghukumar C, Meena RM et al. Fungal diversity in deepsea sediments revealed by culture-dependent and cultureindependent approaches. Fung Ecol 2012;5:543–53.
- Singh P, Raghukumar C, Verma P et al. Fungal community analysis in the deep-sea sediments of the Central Indian Basin by culture-independent approach. Microb Ecol 2011;61:507–17.
- Singh RS, Kaur N, Kennedy JF. Pullulan production from agroindustrial waste and its applications in food industry: a review. Carbohydr Polym 2019;217:46–57.
- Singh R, Gaur R, Biswas P et al. Aureobasidium pullullans, an economically important black yeast. J Basic Appl Mycol 2015;11:1–
- Skropeta D, Wei L. Recent advances in deep-sea natural products. Nat Prod Rep 2014;31:999–1025.
- Sun K, Chen Y, Niu Q et al. An exopolysaccharide isolated from a coral-associated fungus and its sulfated derivative activates macrophages. Int J Biol Macromol 2016;82:387–94.
- Svahn KS, Göransson U, El-Seedi H et al. Antimicrobial activity of filamentous fungi isolated from highly antibiotic-contaminated river sediment. Infect Ecol Epidemiol 2012;2. DOI: 10.3402/iee.v2i0.11591.
- Takami H, Inoue A, Fuji F et al. Microbial flora in the deepest sea mud of the Mariana Trench. FEMS Microbiol Lett 1997;152:279– 85
- Takesako K, Ikai K, Haruna F et al. Aureobasidins, new antifungal antibiotics taxonomy, fermentation, isolation, and properties. J Antibiot (Tokyo) 1991;44:919–24.
- Teske A, de Beer D, McKay LJ et al. The Guaymas Basin hiking guide to hydrothermal mounds, chimneys, and microbial mats: complex seafloor expressions of subsurface hydrothermal circulation. Front Microbiol 2016;7:75. DOI: 10.3389/fmicb.2016.00075.
- Teske A, McKay LJ, Ravelo AC et al. Characteristics and evolution of sill-driven off-axis hydrothermalism in Guaymas Basin the Ringvent site. Sci Rep 2019;9. DOI: 10.1038/s41598-019-50200-5.
- Teske A, Wegener G, Chanton JP et al. Microbial communities under distinct thermal and geochemical regimes in axial and off-axis sediments of Guaymas Basin. Front Microbiol 2021;12:633649. DOI: 10.3389/fmicb.2021.633649.
- Thompson JD, Higgins DG, Gibson TJ. CLUSTAL W: improving the sensitivity of progressive multiple sequence alignment through sequence weighing, position-specific gap penalties and weight matrix choice. *Nucleic Acids Res* 1994;22:4673–80.
- Trinh PTH. Secondary metabolites from a marine-derived fungus Penicillium chrysogenum 045-357-2. Vietnam J Sci Technol 2017;55. DOI: 10.15625/2525-2518/55/1A/12383.
- Uchida N, Mizutani H, Ohshima S et al. Morusin and morusin dimethyl ether. Acta Cryst 1996;52:713–16.
- Vargas-Gastélum L, Riquelme M. The mycobiota of the deep sea: what omics can offer. Life 2020;10:292.
- Wang M, Carver JJ, Phelan VV et al. Sharing and community curation of mass spectrometry data with Global Natural Products Social Molecular Networking. Nat Biotechnol 2016;34:828–38.
- Wang F, Han S, Hu S et al. Two new secondary metabolites from Xylaria sp. cfcc 87468. Molecules 2014;19:1250–57.
- Wang M, Yang L, Feng L et al. Verruculosins A-B, new oligophenalenone dimers from the soft coral-derived fungus Talaromyces verruculosus. Mar Drugs 2019a;17:516.
- Wang Z, Liu Z, Wang Y et al. Fungal community analysis in seawater of the Mariana Trench as estimated by Illumina HiSeq. RSC Adυ 2019b;9:6956–64.

- White T, Bruns T, Lee S et al. 38 -Amplification and direct sequencing of fungal ribosomal RNA genes for phylogenetics. PCR Protoc 1990:315-22.
- Xu W, Luo Z, Guo S et al. Fungal community analysis in the deepsea sediments of the Pacific Ocean assessed by comparison of ITS, 18S and 28S ribosomal DNA regions. Deep Sea Res Part I 2016;**109**:51-60.
- Xu W, Pang K, Luo Z. High fungal diversity and abundance recovered in the deep-sea sediments of the Pacific Ocean. Microb Ecol 2014;68:688-98.
- Xu X, Guo S, Pan KL et al. Fungi associated with chimney and sulfide samples from a South Mid-Atlantic Ridge hydrothermal site: distribution, diversity and abundance. Deep Sea Res Part I 2017;123:48-55.
- Xu X, Ou Z, Wu C. Growth media affect assessment of antimicrobial activity of plant-derived polyphenols. Biomed Res Int 2018a;2018. DOI: 10.1155/2018/8308640.
- Xu W, Gong LF, Pang KL et al. Fungal diversity in deep-sea sediments of a hydrothermal vent system in the Southwest Indian Ridge. Deep Sea Res Part I 2018b;131:16-26.

- Yakti W, Kovács GM, Franken P. Differential interaction of the dark septate endophyte Cadophora sp. and fungal pathogens in vitro and in planta. FEMS Microbiol Ecol 2019;5:fiz164.
- Yan L, Ye D, Chen X et al. Breviane spiroditerpenoids from an extreme-tolerant Penicillium sp. isolated from a deep sea sediment sample. J Nat Prod 2009;72:912-16.
- Yao Q, Wang J, Zhang X et al. Cytotoxic polyketides from the deep-sea-derived fungus Engyodontium album DFFSCS021. Mar Drugs 2014;12:5902-15.
- Yunianto P, Rusman Y, Saepudin E et al. Alkaloid (meleagrine and chrysogine) from endophytic fungi (Penicillium sp.) of Annona squamosa L. PJBS 2014;17:667–74.
- Zalar P, Gunde-Cimerman N. Cold-adapted yeasts in arctic habitats. Berlin: Springer, 2014.
- Zhang XY, Zhang Y, Xu XY et al. Diverse deep-sea fungi from the South China Sea and their antimicrobial activity. Curr Microbiol 2013;67:525-30.
- Zhang X, Tang G, Xu X et al. Insights into deep-sea sediment fungal communities from the East Indian Ocean using targeted environmental sequencing combined with traditional cultivation. PLoS ONE 2014;9:e109118.